PICH regulates the abundance and localization of SUMOylated proteins on mitotic chromosomes

Victoria A. Hassebroek[a], Hyewon Park[a], Nootan Pandey[a], Brooklyn T. Lerbakken[a], Vasilisa Aksenova[b], Alexei Arnaoutov[b], Mary Dasso[b], and Yoshiaki Azuma[a,*]

[a]Department of Molecular Biosciences, University of Kansas, Lawrence, KS 66045; [b]Division of Molecular and Cellular Biology, National Institute of Child Health and Human Development, National Institutes of Health, Bethesda, MD 20892

ABSTRACT **Proper chromosome segregation is essential for faithful cell division and if not maintained results in defective cell function caused by the abnormal distribution of genetic information. Polo-like kinase 1–interacting checkpoint helicase (PICH) is a DNA translocase essential for chromosome bridge resolution during mitosis. Its function in resolving chromosome bridges requires both DNA translocase activity and ability to bind chromosomal proteins modified by the small ubiquitin-like modifier (SUMO). However, it is unclear how these activities cooperate to resolve chromosome bridges. Here, we show that PICH specifically disperses SUMO2/3 foci on mitotic chromosomes. This PICH function is apparent toward SUMOylated topoisomerase IIα (TopoIIα) after inhibition of TopoIIα by ICRF-193. Conditional depletion of PICH using the auxin-inducible degron (AID) system resulted in the retention of SUMO2/3-modified chromosomal proteins, including TopoIIα, indicating that PICH functions to reduce the association of these proteins with chromosomes. Replacement of PICH with its translocase-deficient mutants led to increased SUMO2/3 foci on chromosomes, suggesting that the reduction of SUMO2/3 foci requires the remodeling activity of PICH. In vitro assays showed that PICH specifically attenuates SUMOylated TopoIIα activity using its SUMO-binding ability. Taking the results together, we propose a novel function of PICH in remodeling SUMOylated proteins to ensure faithful chromosome segregation.**

Monitoring Editor
Yukiko Yamashita
University of Michigan

Received: Mar 9, 2020
Revised: Aug 21, 2020
Accepted: Aug 25, 2020

This article was published online ahead of print in MBoC in Press (http://www.molbiolcell.org/cgi/doi/10.1091/mbc.E20-03-0180) on September 2, 2020.

Conflicts of interest: The authors declare no competing financial interests.

Author contributions: V.A.H. conducted almost all of the experiments, created the AID fused PICH cell line and PICH-replaced cell lines, prepared figures, and drafted the manuscript. H.P. prepared DNA constructs for genome editing, created the CRISPR/Cas9 genome edited for inducible expression of the deSUMOylation enzyme and for the Os-TIR1–expressing DLD-1 cell line, created AID fused TopoIIα cell lines, and performed the XEE assay for validation of Py-S2 proteins. N.P. conducted experiments for initial validation of the genome edited cell lines expressing Py-S2. B.T.L. performed initial analysis of immunofluorescent images in Figure 5. V.A., A.A., and M.D. established the AID-mediated degradation system by optimizing the Os-TIR1 integration locus and creating constructs for genome editing by CRISPR/Cas9 for that system. Y.A. designed the study, supervised the project, and wrote the manuscript.

*Address correspondence to: Yoshiaki Azuma (azumay@ku.edu).

Abbreviations used: CSF, cytostatic factor; dnUbc9, dominant negative E2 SUMO-conjugating enzyme; PIAS, protein inhibitor of activated STAT; PICH, Polo-like kinase-interacting checkpoint helicase; SENP, sentrin-specific protease; SIM, SUMO-interacting motif; SPR, strand passage reaction; SUMO, small ubiquitin-like modifier; TopoIIα, topoisomerase IIα; XEE, *Xenopus* egg extract.

INTRODUCTION

Accurate chromosome segregation is a complex and highly regulated process during mitosis. Sister chromatid cohesion is necessary for proper chromosome alignment and is mediated by both cohesin and catenated DNA at centromeric regions (Michaelis *et al.*, 1997; Losada *et al.*, 1998; Bauer *et al.*, 2012). Compared to the well-described regulation of cohesin (Morales and Losada, 2018), the regulation of catenated DNA cleavage by DNA topoisomerase IIα (TopoIIα) is not fully understood despite its critical role in chromosome segregation. ATP-dependent DNA decatenation by TopoIIα takes place during the metaphase-to-anaphase transition, and this allows for proper chromosome segregation (Shamu and Murray, 1992; Wang *et al.*, 2010; Gomez *et al.*, 2014). Failure in resolution of catenanes by TopoIIα leads to the formation of chromosome bridges and ultrafine DNA bridges (UFBs) to which PICH localizes (Spence *et al.*, 2007). PICH is a SNF2 family DNA translocase (Baumann *et al.*, 2007; Biebricher *et al.*, 2013), and its binding to UFBs recruits other proteins to UFBs (Chan *et al.*, 2007; Hengeveld *et al.*, 2015). In addition to the role in UFB binding during anaphase, PICH has been shown to play a key role in chromosome segregation at the metaphase-to-anaphase

transition (Baumann *et al.*, 2007; Nielsen *et al.*, 2015; Sridharan and Azuma, 2016).

Previously, we demonstrated that PICH binds SUMOylated proteins using its three SUMO-interacting motifs (SIMs) (Sridharan *et al.*, 2015). PICH utilizes its ATPase activity to translocate on DNA, similar to known nucleosome-remodeling enzymes (Whitehouse *et al.*, 2003); thus it is a putative remodeling enzyme for chromosomal proteins. But the nucleosome-remodeling activity of PICH was shown to be limited as compared with established nucleosome-remodeling factors (Ke *et al.*, 2011). Therefore, the target of PICH-remodeling activity has not yet been determined. Importantly, both loss of function PICH mutants in either SUMO-binding activity or translocase activity showed chromosome bridge formation (Sridharan and Azuma, 2016), suggesting that both of these activities cooperate to accomplish proper chromosome segregation, albeit the molecular mechanism linking these two functions is unknown. Previous studies demonstrated that proper regulation of mitotic chromosomal SUMOylation is required for faithful chromosome segregation (Nacerddine *et al.*, 2005; Diaz-Martinez *et al.*, 2006; Cubenas-Potts *et al.*, 2013). Studies using *Caenorhabditis elegans* demonstrated the dynamic nature of SUMOylated proteins during mitosis and its critical role in chromosome segregation (Pelisch *et al.*, 2014). Several SUMOylated chromosomal proteins were identified for their potential role in chromosome segregation, for example, TopoIIα, CENP-A, CENP-E, FoxM1, and Orc2 (Bachant *et al.*, 2002; Zhang *et al.*, 2008; Schimmel *et al.*, 2014; Huang *et al.*, 2016; Ohkuni *et al.*, 2018). Because PICH is able to specifically interact with SUMO moieties (Sridharan *et al.*, 2015), these SUMOylated chromosomal proteins could be targets of the SIM-dependent function of PICH in mediating faithful chromosome segregation. Among the known SUMOylated chromosomal proteins, TopoIIα has been shown to functionally interact with PICH. PICH-knockout cells have increased sensitivity to ICRF-193, a potent TopoII catalytic inhibitor, accompanied by increased incidence of chromosome bridges, binucleation, and micronuclei formation (Wang *et al.*, 2008; Kurasawa and Yu-Lee, 2010; Nielsen *et al.*, 2015). ICRF-193 stalls TopoIIα at the last step of the strand passage reaction (SPR) in which two DNA strands are trapped within the TopoIIα molecule without DNA strand breaks (Roca *et al.*, 1994; Patel *et al.*, 2000). In addition to that specific mode of inhibition, ICRF-193 has been shown to increase SUMOylation of TopoIIα (Agostinho *et al.*, 2008; Pandey *et al.*, 2020). Because PICH has SUMO-binding ability, it is possible that increased SUMOylation of TopoIIα contributes to interaction with PICH after ICRF-193 treatment. However, no study has shown a linkage between SUMOylation of TopoIIα and PICH function.

To elucidate possible functional interactions of PICH with SUMOylated chromosomal proteins, we established the connection between PICH and SUMOylation by utilizing specific TopoII inhibitors and genome edited cell lines. Our results demonstrate that increased SUMOylation during ICRF-193 treatment leads to the recruitment and enrichment of PICH on chromosomes. Depletion of SUMOylation abrogates this enrichment, suggesting that PICH specifically targets SUMOylated chromosomal proteins. Depletion of PICH led to the retention of SUMOylated proteins, including SUMOylated TopoIIα on the chromosomes in ICRF-193–treated cells. Replacing endogenous PICH with a translocase-deficient PICH mutant resulted in increased SUMO2/3 foci on chromosomes where PICH was located, suggesting that PICH utilizes its translocase activity to remodel SUMOylated proteins on the chromosomes. In vitro assays showed that PICH specifically interacts with SUMOylated TopoIIα to attenuate SUMOylated TopoIIα activity in a SIM-dependent manner. Taking the results together, we propose a novel mechanism for PICH in promoting proper chromosome segregation during mitosis by remodeling SUMOylated proteins on mitotic chromosomes including TopoIIα.

RESULTS

TopoII inhibitor ICRF-193 induces increased SUMO2/3 modification and increased PICH foci on mitotic chromosomes

We previously reported that PICH utilized its SIMs for proper chromosome segregation and for its mitotic chromosomal localization (Sridharan and Azuma, 2016). We wished to examine whether modulating mitotic SUMOylation affected PICH localization on mitotic chromosomes. Treatment with ICRF-193, a catalytic inhibitor of TopoII that blocks TopoII at the last stage of its SPR, after DNA decatenation but before DNA release, increases SUMO2/3 modification of TopoIIα on mitotic chromosomes. In contrast, treatment with another catalytic TopoII inhibitor, merbarone, which blocks TopoII before the cleavage step of the SPR, does not affect the level of SUMO2/3 modification of TopoIIα (Agostinho *et al.*, 2008; Pandey *et al.*, 2020). We utilized these two contrasting inhibitors to assess whether TopoIIα inhibition and/or SUMOylation changes PICH distribution on mitotic chromosomes. DLD-1 cells were synchronized in prometaphase, mitotic cells were collected by mitotic shake off, and then chromosomes were isolated. To assess the effects of the TopoII inhibitors specifically during mitosis, the inhibitors were added to cells after mitotic shake off. Consistent with previous reports (Agostinho *et al.*, 2008; Pandey *et al.*, 2020), Western blot analysis of isolated chromosomes showed that treatment with ICRF-193 significantly increased the overall SUMO2/3 modification of chromosomal proteins, including SUMOylated TopoIIα (marked by red asterisks in Figure 1A). Intriguingly, a novel finding showed that PICH levels on mitotic chromosomes were significantly increased in cells treated with ICRF-193. In contrast, merbarone did not increase the level of these proteins on the chromosomes, suggesting that there is a specificity of ICRF-193 inducing increased levels of PICH and SUMOylation of TopoIIα (Figure 1A).

To investigate the localization of PICH on mitotic chromosomes treated with ICRF-193, mitotic cells were subjected to immunofluorescence staining. Synchronized cells were collected by mitotic shake off, treated with inhibitors for 20 min, and then plated onto fibronectin-coated coverslips. As seen in Western blot analysis, increased intensity of SUMO2/3 foci were observed on the chromosomes, where they overlapped with TopoIIα foci upon ICRF-193 treatment (Figure 1B, enlarged images). Although the TopoIIα signal changed during merbarone treatment, showing a less punctate signal, no enrichment of SUMO2/3 foci was observed (Figure 1B). A novel observation showed that treatment with ICRF-193 caused a redistribution of PICH from all over the chromosomes to an enrichment at foci on the chromosomes where they overlapped with the SUMO2/3 foci (Figure 1C, enlarged images). Treatment with merbarone did not affect PICH localization (Figure 1C). By outlining single chromosomes using the DNA signal in multiple images and then placing outlines on SUMO2/3 or TopoIIα channels, the mean intensities of these signals were measured. Both TopoIIα and SUMO2/3 chromosome signal intensities were significantly higher after ICRF-193 treatment, but not in merbarone-treated cells (Figure 1D). PICH foci intensity was measured by using circles equal in size; the PICH foci intensity was found to be significantly increased in ICRF-193–treated cells (Figure 1D, bottom graph). These data show that treatment with ICRF-193, but not merbarone, induces increased TopoIIα SUMOylation and enrichment of PICH and SUMO2/3 foci on the chromosomes.

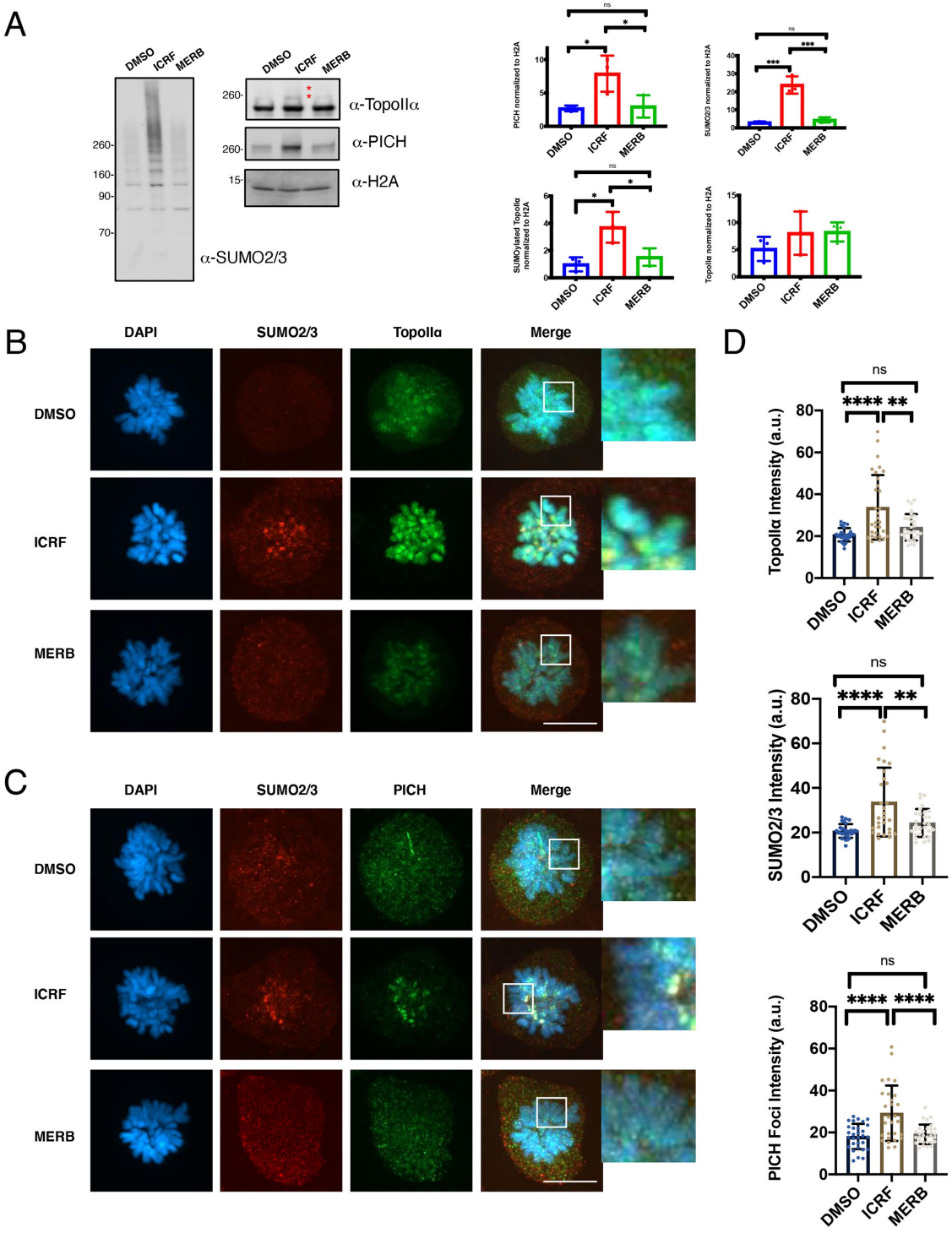

FIGURE 1: TopoIIα inhibition by ICRF-193 leads to increased PICH, SUMO2/3, and TopoIIα levels on mitotic chromosomes. (A) DLD-1 cells were synchronized and treated with the indicated inhibitors (7 μM ICRF-193: ICRF and 40 μM merbarone: MERB); DMSO was used as a control. Mitotic chromosomes were isolated and subjected to Western blotting with the indicated antibodies. Intensity of signals (arbitrary unit; a.u.) normalized by H2A are shown with mean value and SD. * indicates SUMOylated TopoIIα. *p* values for comparison from three experiments were calculated using a one-way ANOVA with Tukey multicomparison correction. ns: not significant; *: $p \leq 0.05$; ***: $p < 0.001$. (B) Mitotic cells treated with DMSO (control), ICRF-193, and merbarone were stained with antibodies against TopoIIα (green) and SUMO2/3 (red). DNA was stained with DAPI (blue). Scale bar = 11 μm. The white square indicates enlarged area. (C) Mitotic cells were treated as in B and stained with antibodies against PICH (green) and SUMO2/3 (red). DNA was stained with DAPI (blue). Scale bar = 11 μm. The white square indicates enlarged area. (D) Using DAPI signal the mean intensities (a.u.) of each channel of at least five individual chromosomes per experimental replicate were measured. The bar indicates the mean value of the intensities. *p* values for comparison of all obtained values from three experiments were calculated using a one-way ANOVA with Tukey multicomparison correction ns: not significant; **: $p < 0.01$; ****: $p < 0.0001$.

SUMOylation is required for PICH enrichment in ICRF-193–treated cells

Although results obtained from inhibiting TopoIIα suggest that increased SUMOylation plays a critical role in PICH enrichment, the distinct effects of the different inhibitor treatments, for example, differences in TopoII conformation, could also play a role. To determine whether mitotic SUMOylation is critical for PICH enrichment in ICRF-193–treated cells, we developed a novel method to inhibit mitotic SUMOylation in cells. First, we generated a fusion protein, called Py-S2, which consists of the N-terminal region of human PIASy and the SENP2-catalytic domain (required for deSUMOylation) (Reverter and Lima, 2004; Ryu *et al.*, 2015; Sridharan *et al.*, 2015). The N-terminal region of PIASy localizes to mitotic chromosomes, in part via its specific interaction with the RZZ (Rod-Zw10-Zwilch) complex (Ryu and Azuma, 2010). Thus, the fusion protein is expected to bring deSUMOylation activity where mitotic SUMOylation occurs on chromosomes by PIASy. As a negative control, we substituted a cysteine to alanine at position 548 of SENP2 (called Py-S2 Mut) to create a loss of function mutant (Reverter and Lima, 2004, 2006) (Figure 2A). The activity of the recombinant fusion proteins on chromosomal SUMOylation was verified in *Xenopus* egg extract (XEE) assays (Supplemental Figure S1). As predicted, the addition of Py-S2 protein to XEE completely eliminated mitotic chromosomal SUMOylation. To our surprise, the Py-S2 Mut protein stabilized SUMOylation of chromosomal proteins, thus acting as a dominant negative mutant against endogenous deSUMOylation enzymes. To express the fusion proteins in cells, we created inducible expression cell lines using the tetracycline-inducible system (Supplemental Figure S2) (Natsume *et al.*, 2016). We utilized CRISPR/Cas9 genome editing to integrate each of the fusion genes into the human H11 (hH11) safe harbor locus (Zhu *et al.*, 2014; Ruan *et al.*, 2015) in DLD-1 cells.

To test whether the Py-S2 fusion protein worked as expected, cells were synchronized and doxycycline was added after release from a thymidine block. After treatment with ICRF-193, chromosomes were isolated and subjected to Western blot analysis. The Py-S2–expressing cells had nearly undetectable levels of chromosomal SUMOylation as well as SUMOylated TopoIIα (Figure 2B). Intriguingly in Py-S2–expressing cells, PICH levels on chromosomes no longer showed a significant increase under ICRF-193 treatment, suggesting that the response of PICH to ICRF-193 depends on the cell's ability to SUMOylate chromosomal proteins (Figure 2B, quantification). The role of SUMOylation in the enrichment of PICH on mitotic chromosomes is further supported by the Py-S2 Mut–expressing cells. Western blot analysis of mitotic chromosomes expressing Py-S2 Mut revealed a slight increase in overall SUMOylation levels in the absence of ICRF-193 (Figure 2C, lane 1 vs. lane 3, quantification). But SUMOylated TopoIIα did not show a significant increase in either control or ICRF-193–treated conditions. This suggests that a similar stabilization of SUMOylation occurs in cells as was observed in the XEE assays, albeit with less penetrance. PICH levels were also slightly increased in the Py-S2 Mut–expressing cells in the absence of ICRF-193 (Figure 2C, lane 1 vs. lane 3, quantification).

To determine how deSUMOylation affects PICH and SUMO2/3 distribution on chromosomes, Py-S2–expressing mitotic cells were subjected to immunofluorescence staining. Immunofluorescence analysis of Py-S2–expressing cells reiterated what was observed in Western blot analysis. By utilizing the same quantification methodology as in Figure 1, measuring individual chromosome mean intensities, we saw that even under ICRF-193 treatment, Py-S2–expressing cells displayed significantly lower levels of SUMO2/3 signals on chromosomes (Figure 3A, quantification). Then the distribution of the SUMO2/3 signal was assessed by calculating the ratio of SUMO2/3 foci intensity divided by the total intensity (hereafter this analysis will be referred to as "granularity" as marked on each graph). The results showed that expression of Py-S2 completely diminishes the enrichment of SUMO2/3 foci even after ICRF-193 treatment. PICH chromosomal intensity was also reduced in Py-S2–expressing cells, where no significant change in intensity or distribution occurred upon ICRF-193 treatment (Figure 3B, quantification). But total TopoIIα signals remained unaffected by inhibition of SUMOylation, agreeing with our previous observations in XEE assays (Azuma *et al.*, 2005) (Figure 3C, quantification). By measuring TopoIIα granularity, the enrichment of TopoIIα foci with ICRF-193 treatment was still observed, suggesting that ICRF-193 treatment affects the distribution of TopoIIα independent of SUMOylation. Next the Py-S2 Mut–expressing cells were analyzed to examine the effect of stabilizing SUMOylation. The increase of both PICH and SUMO2/3 signals observed in Western blot quantification was also apparent with immunofluorescence analysis. In control cells (dimethyl sulfoxide [DMSO]) expressing Py-S2 Mut, both total SUMO2/3 intensity and granularity on chromosomes showed a significant increase. No additive effects were observed with ICRF-193 treatment in either total intensity or granularity (Figure 4A, quantifications). The discrepancy between Western blot data (Figure 2C) and quantification of immunofluorescence images implies that these increased SUMO2/3-modified proteins could be lost from chromosomal fractions during the isolation process for Western blotting. Intriguingly, in control cells (DMSO) expressing Py-S2 Mut, we observed increased chromosomal PICH intensity as compared with ICRF-193–treated Py-S2 Mut–expressing cells (Figure 4B, quantification), which mirrors the SUMO2/3 total intensity result. PICH granularity was not clearly increased by ICRF-193 treatment in Py-S2 Mut–expressing cells, and this also mirrors the SUMO2/3 granularity results. Similar to Figure 3C, TopoIIα signal intensity did not change upon Py-S2 Mut expression (Figure 4C, quantification). However, TopoIIα granularity is increased by expression of Py-S2 Mut without ICRF-193, suggesting that increased SUMO2/3 modification on chromosomes affects the chromosomal distribution of TopoIIα. In all, these data reinforce the indication that chromosomal SUMOylation plays a critical role in the enrichment of chromosomal PICH localization, including PICH foci formation in ICRF-193–treated cells.

Increased PICH levels observed after ICRF-193 treatment are lost upon TopoIIα depletion

ICRF-193 treatment led to a distinct enrichment of SUMO2/3 and PICH foci unlike simply stabilizing SUMO2/3 modification on chromosomal proteins by Py-S2 Mut expression. Therefore, we tested whether the PICH response to ICRF-193 is due to TopoIIα SUMOylation. To accomplish this, we generated an mAID-TopoIIα cell line that enables rapid and complete elimination of TopoIIα in the presence of auxin (Nishimura *et al.*, 2009; Natsume *et al.*, 2016). First, we established a cell line that has an integration of an auxin-dependent ubiquitin E3 ligase, *OsTIR1* gene, at the promoter of a housekeeping (*RCC1)* gene (Supplemental Figure S3, A–C) using CRISPR/Cas9 editing technology (Yau *et al.*, 2020). The integration of the *OsTIR1* gene under the *RCC1* promoter achieved stable and low-level expression of the protein and thus minimized the nonspecific degradation of AID-tagged proteins without auxin. Using the established OsTIR1-expressing DLD-1 cell line, DNA encoding a mAID-Flag tag was inserted into both TopoIIα loci (Supplemental Figure S4, A–C). After 6-h treatment with auxin, TopoIIα was degraded to undetectable levels in all cells analyzed (Supplemental Figure S4, D and E). This rapid elimination allowed us to examine the effect of TopoIIα depletion in a single cell cycle.

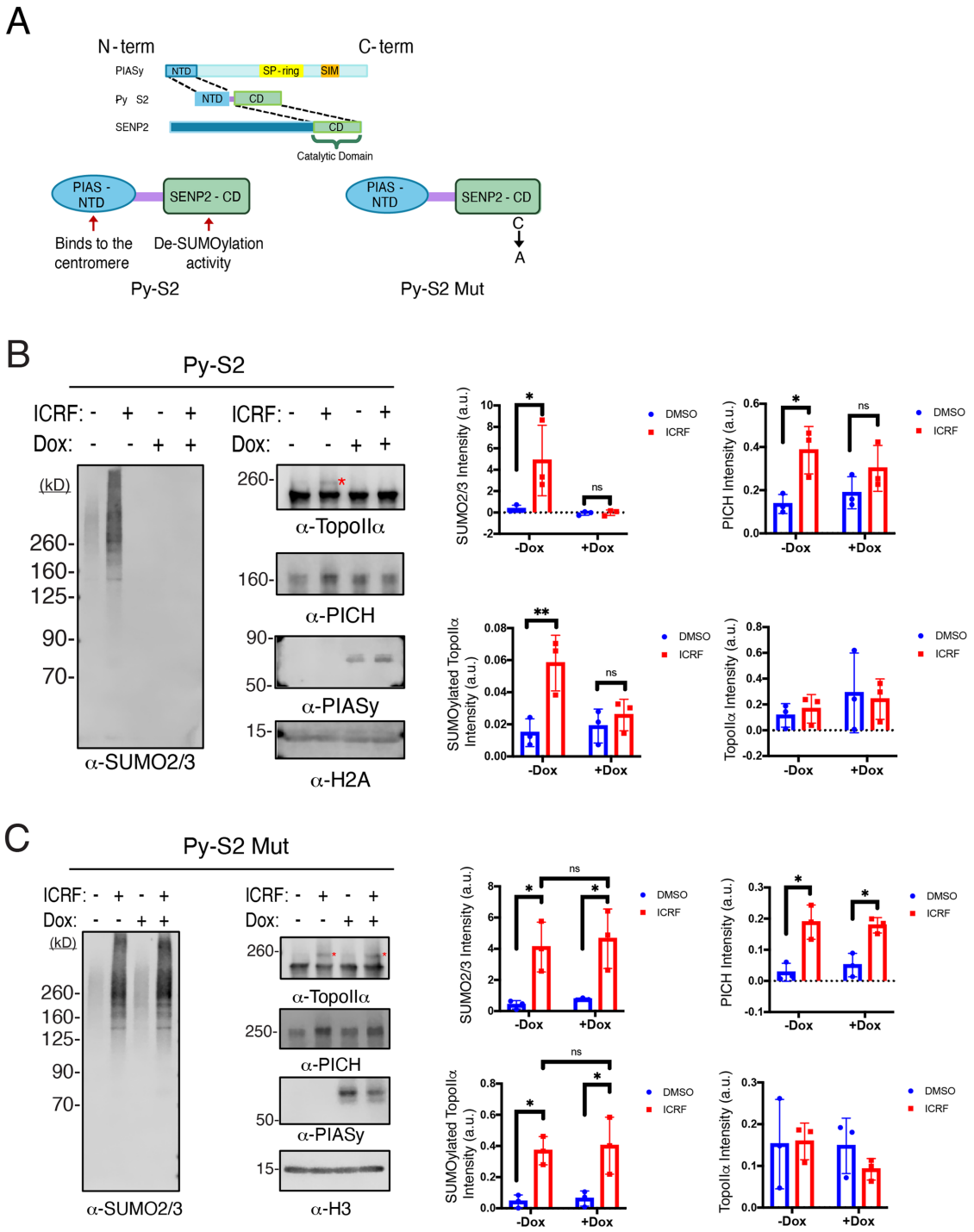

FIGURE 2: Modulating chromosomal SUMOylation affects chromosomal binding of PICH. (A) Schematic of fusion proteins generated for modulating SUMOylation on mitotic chromosomes. (B) Py-S2–expressing or nonexpressing mitotic chromosomes were subjected to Western blotting with the indicated antibodies. * indicates SUMOylated TopoIIα. Intensities of signals (a.u.) normalized by H2A are shown with mean value and SD. *p* values for comparison from three experiments were calculated using a two-way ANOVA with Tukey multicomparison correction; ns: not significant; *: $p \leq 0.05$; **: $p < 0.01$. (C) Py-S2 Mut–expressing or nonexpressing mitotic chromosomes were isolated and subjected to Western blotting with the indicated antibodies. * indicates SUMOylated TopoIIα. Intensities of signals (a.u.) normalized by H3 are shown with mean value with SD. *p* values for comparison among three experiments were calculated using a two-way ANOVA with Tukey multicomparison correction. ns: not significant; *: $p \leq 0.05$.

To deplete TopoIIα, the cells were treated with auxin after release from a thymidine block. After mitotic shake off and treatment with ICRF-193, isolated chromosomes were subjected to Western blotting with anti-SUMO2/3, anti-TopoIIα, and anti-PICH antibodies, and anti-H2A was used as a loading control. A slight overall increase of global SUMOylation was still observed in ΔTopoIIα cells treated with ICRF-193. This suggests that ICRF-193 affects SUMOylation of other chromosomal proteins, such as TopoIIβ (Figure 5A). Notably,

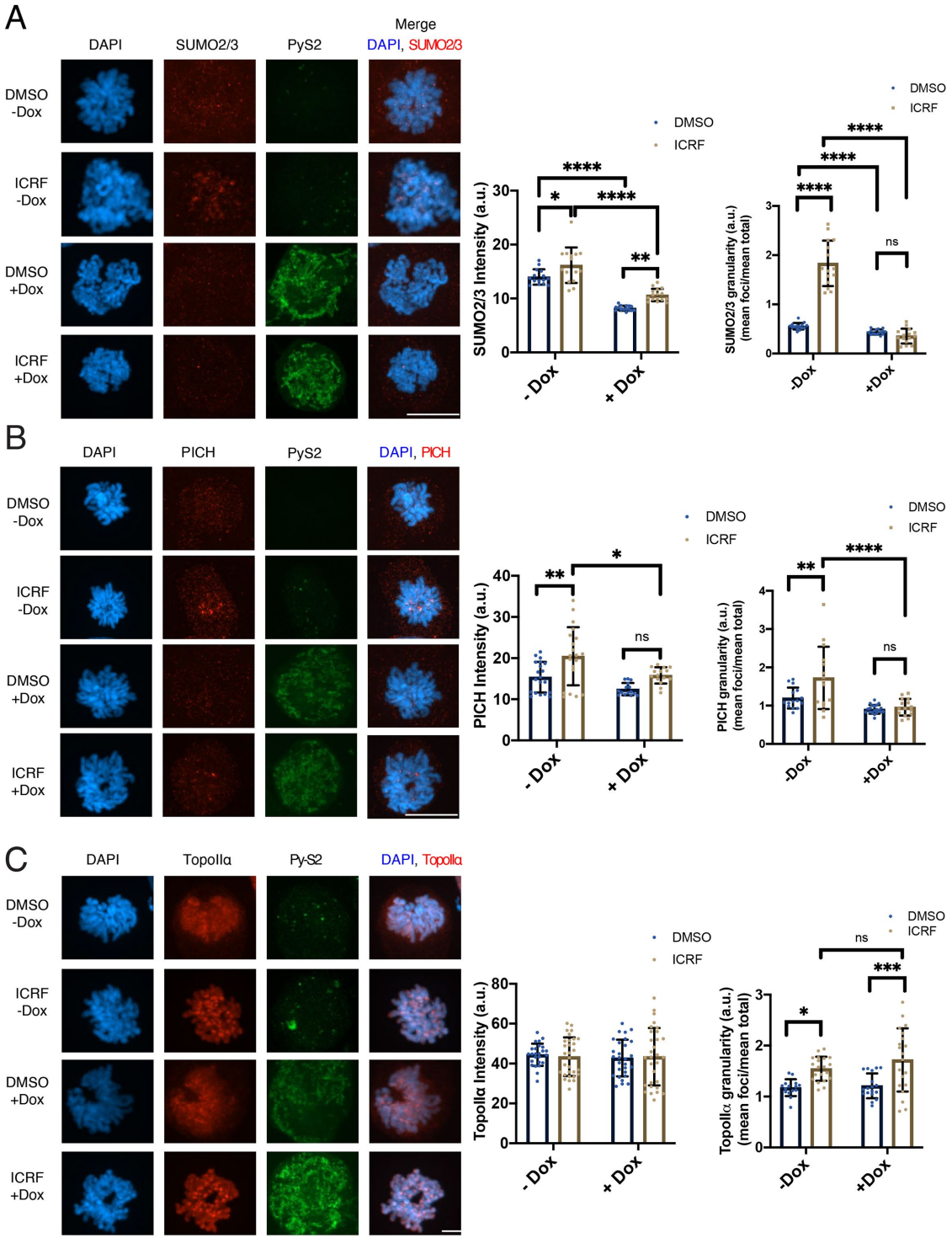

FIGURE 3: Decreased mitotic SUMOylation eliminates PICH response to ICRF-193. (A) Mitotic cells were fixed and stained with antibodies against SUMO2/3 (red) and mNeon (green). DNA was stained by DAPI (blue). Scale bar = 11 μm. The mean intensities of SUMO2/3 signals are shown. *p* values for comparison of all obtained values from three experiments were calculated using a two-way ANOVA with Tukey multicomparison correction; ns: not significant; *: $p \leq 0.05$; ****: $p < 0.0001$. (B) Mitotic cells were fixed and stained with antibodies against PICH (red) and mNeon (green). DNA was stained by DAPI (blue). Scale bar = 11 μm. The mean intensities of PICH signals are shown. *p* values for comparison of all obtained values from three experiments were calculated using a two-way ANOVA with Tukey multicomparison correction; ns: not significant; *: $p \leq 0.05$; **: $p < 0.01$; ****: $p < 0.0001$. (C) Mitotic cells were fixed and stained with antibodies against TopoIIα (red) and mNeon (green). DNA was stained by DAPI (blue). Scale bar = 11 μm. The mean intensities of TopoIIα signals are shown. *p* values for comparison of all obtained values from three experiments were calculated using a two-way ANOVA with Tukey multicomparison correction; ns: not significant; *: $p \leq 0.05$; ***: $p < 0.001$.

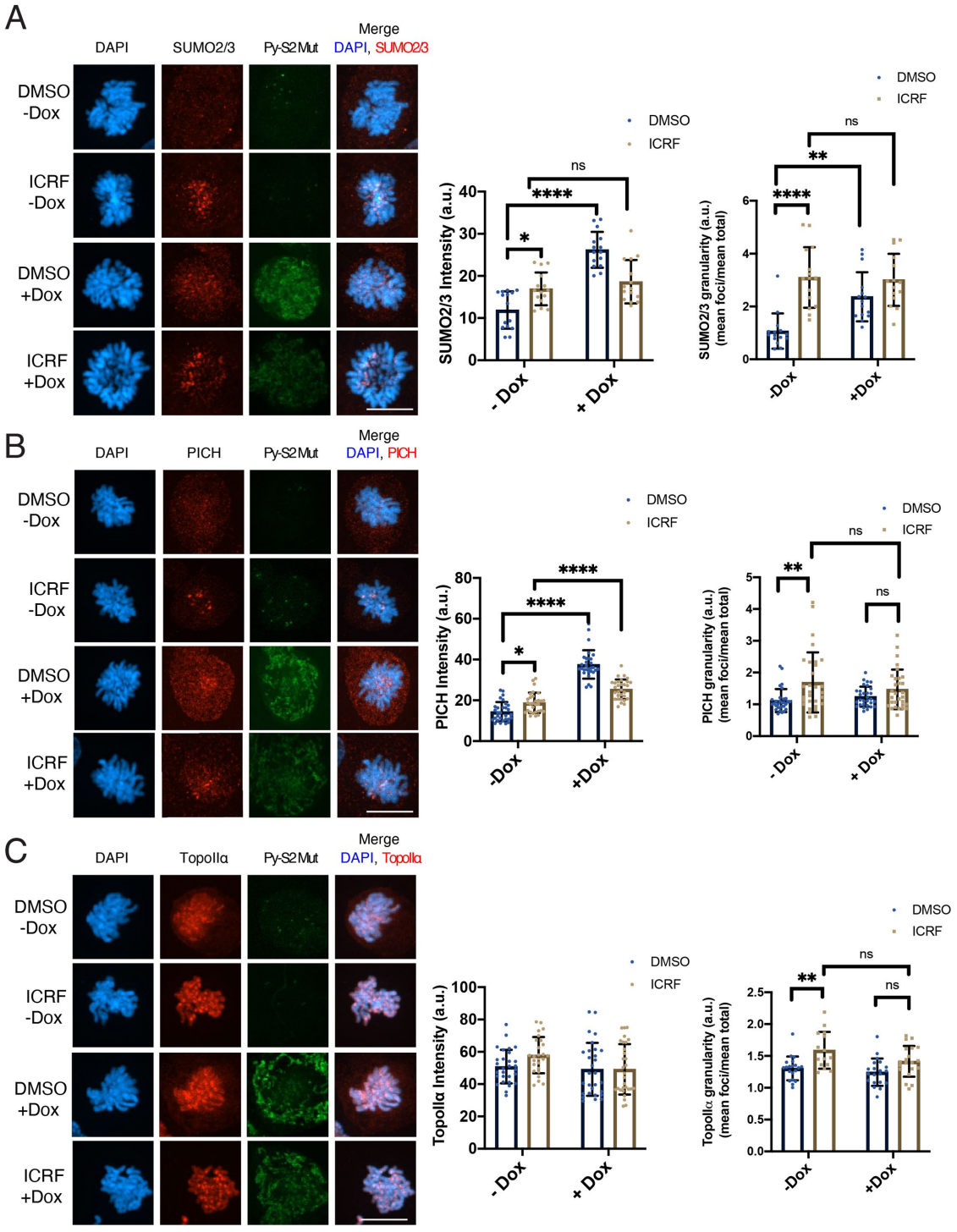

FIGURE 4: Mutant form of deSUMOylation enzyme promotes PICH and SUMO2/3 foci in both control and ICRF-193–treated cells. (A) Mitotic cells were fixed and stained with antibodies against SUMO2/3 (red) and mNeon (green). DNA was stained by DAPI (blue). Scale bar = 11 μm. The mean intensities of SUMO2/3 signals are shown. *p* values for comparison of all obtained values from three experiments were calculated using a two-way ANOVA with Tukey multicomparison correction; ns: not significant; *: $p \leq 0.05$; **: $p < 0.01$; ****: $p < 0.0001$. (B) Mitotic cells were fixed and stained with antibodies against PICH (red) and mNeon (green). DNA was stained by DAPI (blue). Scale bar = 11 μm. The mean intensities of PICH signals are shown. *p* values for comparison of all obtained values from three experiments were calculated using a two-way ANOVA with Tukey multicomparison correction; ns: not significant; *: $p \leq 0.05$; **: $p < 0.01$; ****: $p < 0.0001$. (C) Mitotic cells were fixed and stained with antibodies against TopoIIα (red) and mNeon (green). DNA was stained by DAPI (blue). Scale bar = 11 μm. The mean intensities of TopoIIα signals are shown. *p* values for comparison of all obtained values from three experiments were calculated using a two-way ANOVA with Tukey multicomparison correction; ns: not significant; **: $p < 0.01$.

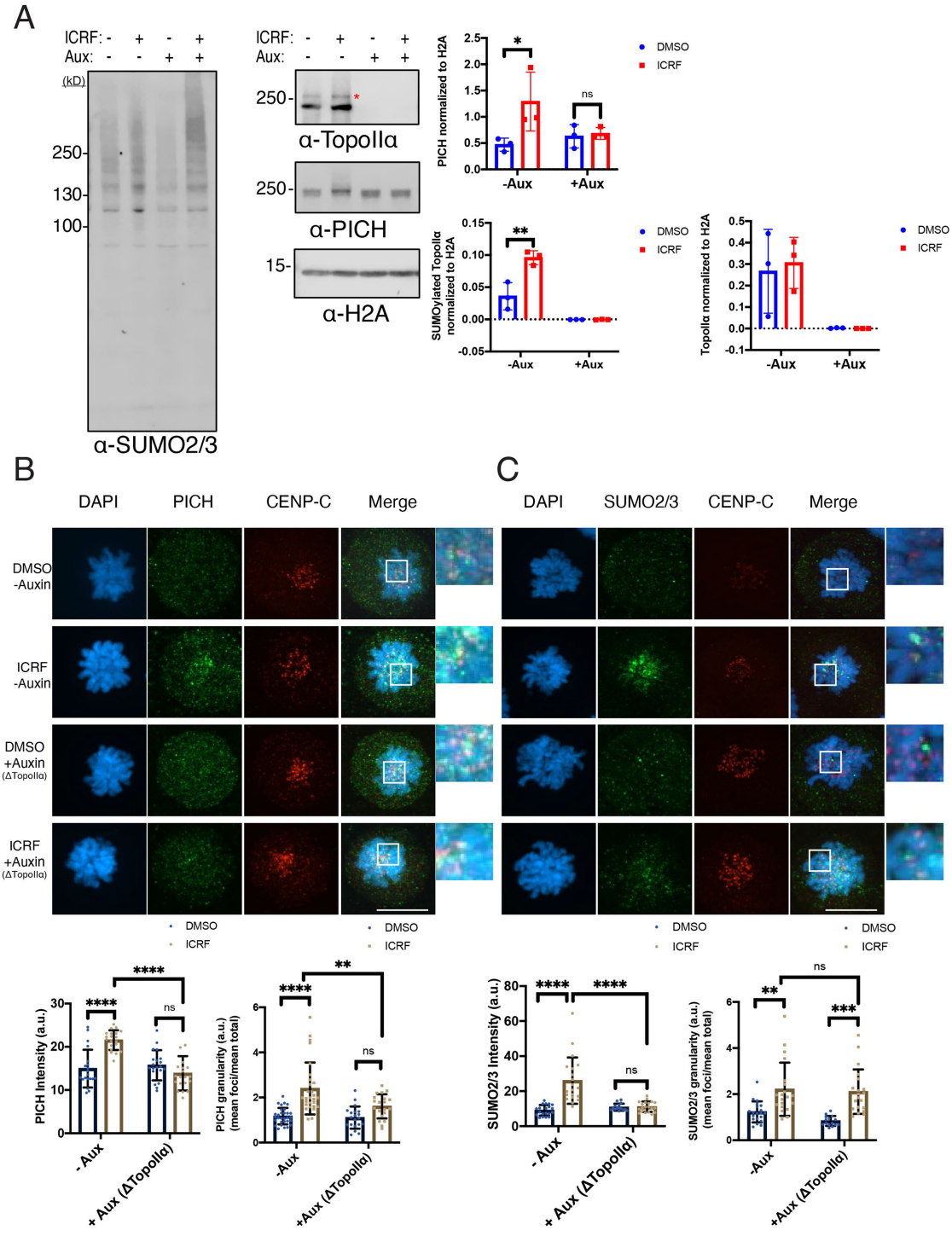

FIGURE 5: Depletion of TopoIIα attenuates SUMO2/3 modification and eliminates PICH response in ICRF-193–treated cells. (A) DLD-1 cells with endogenous TopoIIα tagged with a mAID were synchronized in mitosis and treated with DMSO (control) and ICRF-193. Auxin was added to the cells after release from thymidine for 6 h. Mitotic chromosomes were isolated and subjected to Western blotting with the indicated antibodies. * indicates SUMOylated TopoIIα. Intensities of signals (a.u.) normalized by H3 are shown with mean values and SD. *p* values for comparison from three experiments were calculated using a two-way ANOVA with Tukey multicomparison correction; ns: not significant; *: $p \leq 0.05$; **: $p < 0.01$. (B) Mitotic cells were fixed and stained with antibodies against PICH (green) and CENP-C (red). DNA was stained with DAPI (blue). Scale bar = 11 μm. The white square indicates enlarged area. The mean intensities of PICH signals are shown. *p* values for comparison of all obtained values from three experiments were calculated using a two-way ANOVA with Tukey multicomparison correction; ns: not significant; **: $p < 0.01$; ****: $p < 0.0001$. (C) Mitotic cells were fixed and stained with antibodies against SUMO2/3 (green) and CENP-C (red). DNA was stained with DAPI (blue). Scale bar = 11 μm. The white square indicates enlarged area. The mean intensities of SUMO2/3 signals are shown. *p* values for comparison of all obtained values from three experiments were calculated using a two-way ANOVA with Tukey multicomparison correction; ns: not significant; **: $p < 0.01$; ***: $p < 0.001$; ****: $p < 0.0001$.

ΔTopoIIα cells treated with ICRF-193 showed no changes in PICH levels on the chromosomes. This suggests that increased levels of PICH seen in ICRF-193 treatment is a SUMOylated TopoIIα-dependent response (Figure 5A). Immunofluorescence analysis of PICH showed fewer foci on the chromosomes after ICRF-193 treatment in ΔTopoIIα cells as compared with cells with intact TopoIIα treated with ICRF-193. This observation was quantified by measuring the PICH chromosomal signal intensity, which showed a statistically significant decrease in mean PICH intensity in ICRF-193–treated ΔTopoIIα cells (Figure 5B, quantification). Further, measuring the centromeric PICH foci intensity and calculating the ratio of centromeric PICH among total PICH on chromosomes (Figure 5B, granularity quantification) revealed that when TopoIIα is depleted in cells, ICRF-193 treatment did not increase PICH. Similarly, ΔTopoIIα cells showed a significant decrease in SUMO2/3 chromosome signal intensity even under ICRF-193 treatment (Figure 5C, quantification). The discrepancy from Western blotting analysis (Figure 5A) could originate from the extraction conditions of the chromosome samples as indicated in the Py-S2 Mut section (Figures 2C and 4B). However, centromeric SUMO2/3 granularity was still significantly increased in ΔTopoIIα cells with ICRF-193 (SUMO2/3 granularity quantification), indicating that other proteins located at the centromere were still modified under ICRF-193 treatment and these were not significantly contributing to PICH enrichment at centromeres. These results suggest that TopoIIα SUMOylation critically contributes to the centromeric enrichment of PICH on chromosomes under ICRF-193 treatment.

Loss of PICH leads to enrichment of chromosomal SUMOylated proteins

So far, the results indicate that PICH is recruited to SUMOylated chromosomal proteins, in particular SUMOylated centromeric TopoIIα in ICRF-193–treated cells. Because the ability of PICH to interact with SUMO via its SUMO-interacting motifs is required for proper chromosome segregation, we wished to determine whether PICH is required for regulating the association of SUMOylated proteins with chromosomes. To examine this, mAID-PICH cells were generated as described above for TopoIIα. After auxin was added to the cells for 6 h, PICH levels became undetectable by Western blot and immunofluorescence analysis (Supplemental Figure S5, A–E). To deplete PICH, auxin was added to the cells after release from a thymidine block, and then mitotic cells were collected by mitotic shake off. Isolated chromosomes were then subjected to Western blot analysis. Intriguingly, compared with cells treated with DMSO (control) and no auxin, ΔPICH control cells showed an increase in SUMOylated TopoIIα, revealed by the appearance of a second upshifted band marked by an asterisk (Figure 6A). In addition, Western blots showed that cells depleted for PICH and treated with DMSO (control) showed an overall increase in SUMO2/3 signal, although not statistically significant (Figure 6A, compare lanes 1 and 3). Immunofluorescence staining further supported this novel role of PICH on SUMOylated chromosomal proteins. ΔPICH cells stained for SUMO2/3 showed a significant increase in mean chromosomal intensity as compared with control cells with intact PICH (Figure 6B, quantification). In ΔPICH cells treated with ICRF-193, the intensity of chromosomal SUMO2/3 was not significantly higher than in cells with intact PICH. In addition, centromeric SUMO2/3 granularity showed that depletion of PICH increased centromeric SUMO2/3 foci intensity on chromosomes, which was further increased under ICRF-193 treatment (Figure 6B, granularity quantification). This suggests that PICH acts on SUMO2/3-modified chromosomal proteins to attenuate their binding to chromosomes, including centromeric enrichment in both control and ICRF-193–treated conditions. The discrepancy between Western blot and immunofluorescence image quantification suggests that these stabilized SUMO2/3-modified proteins on chromosomes after PICH depletion are rather weakly associated with chromosomes and likely dissociate during biochemical isolation similar to Py-S2 Mut–expressing cells. As compared with control cells (DMSO) with intact PICH, ΔPICH cells treated with DMSO showed a significant increase of mean TopoIIα chromosomal intensity and granularity (Figure 6C, quantification). ICRF-193 treatment did not further increase total TopoIIα intensity. The granularity of centromeric TopoIIα in ΔPICH cells after DMSO and ICRF-193 treatment was lower than that of cells with PICH. Together, the results suggest that PICH functions in the regulation and proper localization of SUMOylated chromosomal proteins and TopoIIα at the centromere.

ATP-dependent translocase activity and SIMs of PICH are required for regulating SUMOylated chromosomal proteins

To identify which function of PICH is required for the chromosomal distribution of SUMOylated proteins, we created a PICH-replacement cell line by combining mAID-mediated PICH depletion and inducible expression of exogenous PICH mutants. The mAID-PICH cells had CRISPR/Cas9-targeted integration of either Tet-inducible WT PICH-mCherry, an ATPase dead mutant (K128A-mCherry), or a non–SUMO-interacting form of PICH (d3SIM-mCherry) into the CCR5 safe harbor locus (Papapetrou and Schambach, 2016). After clonal isolation and validation (Supplemental Figure S6, A–C), PICH-mCherry expression was tested in asynchronous cells by treatment with auxin and doxycycline for 14 h, and the whole cell lysates were used for Western blot analysis. Although the expression level of the exogenous proteins was variable, we were able to replace endogenous PICH with exogenous PICH (Figure 7A). We did observe variation of mCherry expression within each clonal isolate (Supplemental Figure S6D), and this may explain the variation in expression levels observed in Western blot analysis. The PICH replacement for mitotic cell analysis was achieved by incubating cells with auxin or auxin and doxycycline for 22 h before mitotic shake off. The mitotic cells were treated with DMSO (control) or ICRF-193, and then mitotic chromosomes were isolated. Western blot analysis was performed to determine how translocase activity and SIMs contribute to PICH-binding mitotic chromosomes (Figure 7B). The PICH WT-mCherry was observed to have a response to ICRF-193 similar to that of endogenous PICH, showing increased binding with ICRF-193 treatment. The K128A mutant also showed increased binding after ICRF-193 treatment. In contrast, the d3SIM mutant could not bind to chromosomes. This suggests that PICH SIMs are required for chromosomal association, which is consistent with our previous observations (Sridharan and Azuma, 2016).

To further examine how the PICH mutants affect chromosomal localization of SUMO2/3 and TopoIIα, immunofluorescence analysis of prometaphase cells was performed. PICH WT-mCherry showed the same staining patterns as endogenous PICH, and its response to ICRF-193 was similar to that in Figure 1. Both SUMO2/3 and TopoIIα total intensities increased in response to ICRF-193 treatment. Distribution analysis also showed increased granularity for both SUMO2/3 and TopoIIα under ICRF-193 treatment. But TopoIIα granularity was not statistically significantly increased in PICH WT-mCherry–replaced cells. This discrepancy likely originates from the limitations of the system in terms of control of expression levels of transgenes. Loss of PICH showed increased TopoIIα granularity (Figure 6C); thus insufficient expression of PICH WT-mCherry could affect the TopoIIα ability to form foci.

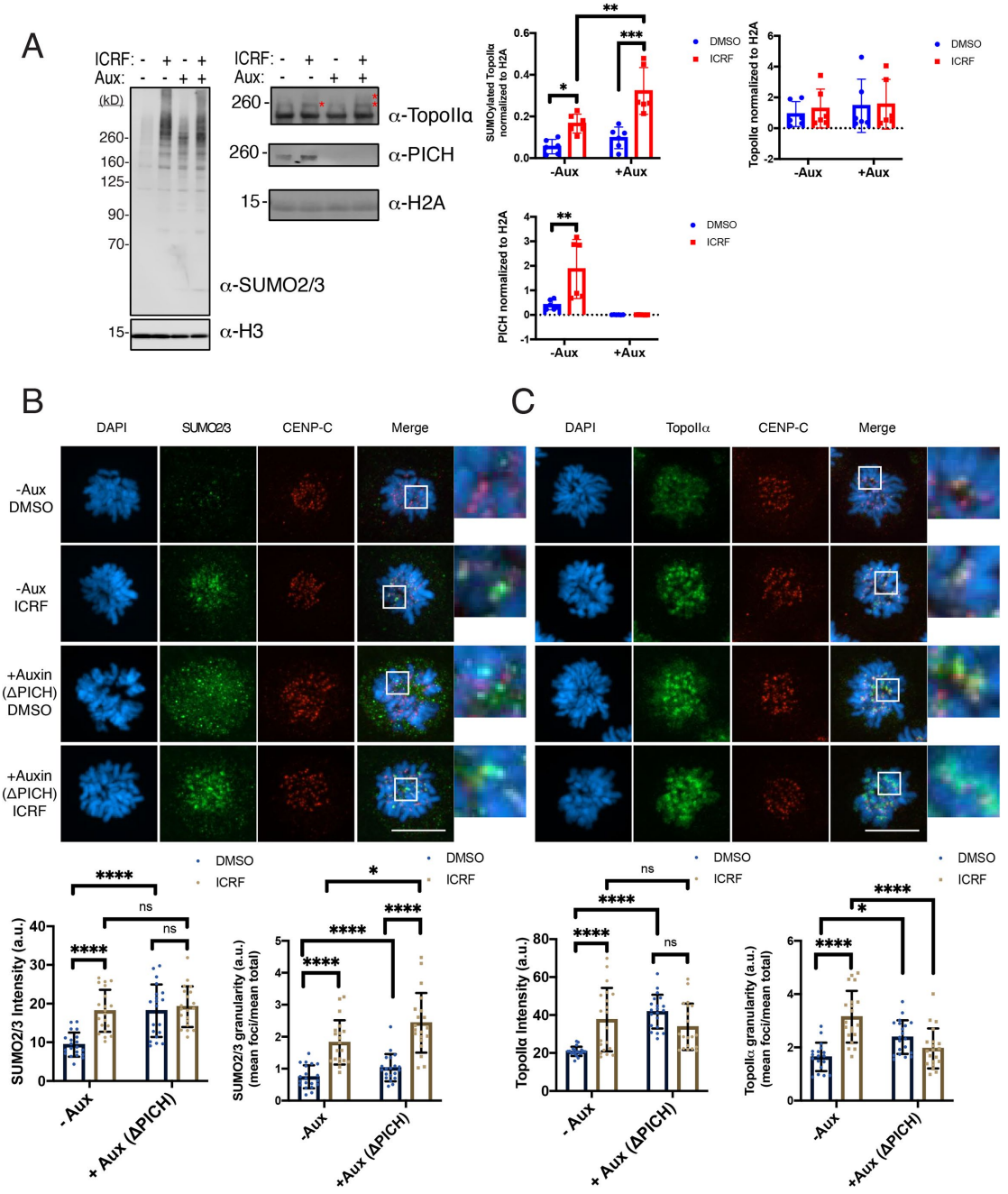

FIGURE 6: PICH-depleted chromosomes show increased levels of SUMOylated TopoIIα. (A) DLD-1 cells with endogenous PICH tagged with a mAID were synchronized in mitosis and treated with DMSO (control) and ICRF-193. Auxin was added to the cells after release from thymidine for 6 h. Mitotic chromosomes were isolated and subjected to Western blotting with the indicated antibodies. * indicates SUMOylated TopoIIα. Intensities of signals (a.u.) normalized by H2A are shown with mean value and SD. *p* values for comparison from three experiments were calculated using a two-way ANOVA and Tukey multicomparison correction; ns: not significant; *: $p \leq 0.05$; **: $p < 0.01$; ***: $p < 0.001$. (B) Mitotic cells were fixed and stained with antibodies against SUMO2/3 (green) and CENP-C (red). DNA was stained with DAPI (blue). Scale bar = 11 μm. The white square indicates enlarged area. The mean intensities of SUMO2/3 signals are shown. *p* values for comparison of all obtained values from three experiments were calculated using a two-way ANOVA and Tukey multicomparison correction; ns: not significant; *: $p \leq 0.05$; ****: $p < 0.0001$. (C) Mitotic cells were fixed and stained with antibodies against TopoIIα (green) and CENP-C (red). DNA was stained with DAPI (blue). Scale bar = 11 μm. The white square indicates enlarged area. The mean intensities of TopoIIα signals are shown. *p* values for comparison of all obtained values from three experiments were calculated using a two-way ANOVA and Tukey multicomparison correction; ns: not significant; *: $p \leq 0.05$; ****: $p < 0.0001$.

Despite the limitation of expression-level control, the results support the feasibility of this system to assess PICH function by replacing the endogenous PICH with mutants.

When the K128A mutant, which cannot translocate DNA, was expressed, strong mCherry foci were observed on the chromosomes regardless of ICRF-193 treatment. Importantly, these foci

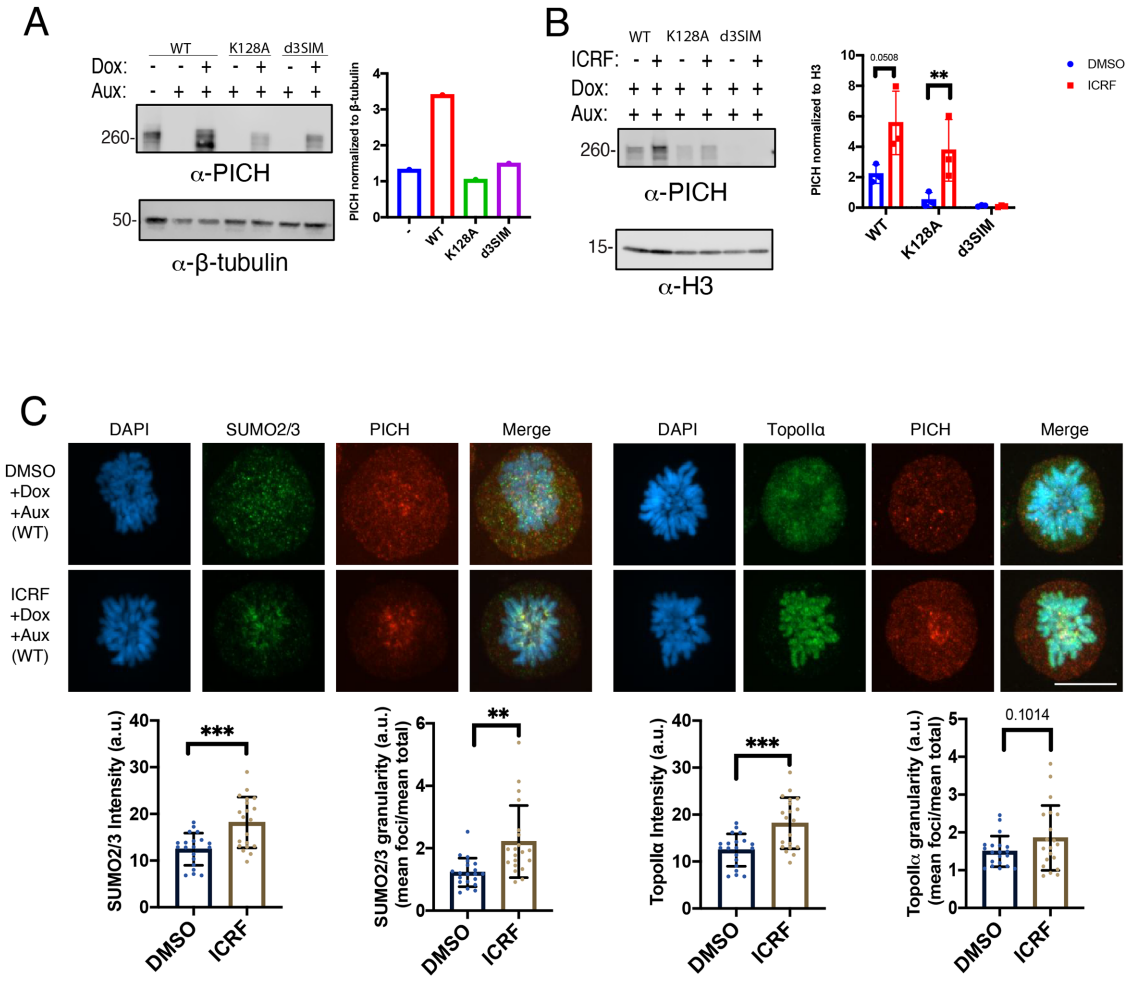

FIGURE 7: Expression of exogenous mCherry-tagged PICH functions similarly to endogenous PICH. (A) DLD-1 cells with endogenous PICH tagged with a mAID and exogenous PICH mCherry mutants were treated with auxin or auxin and doxycycline for 14 h. Whole cell lysates were subjected to Western blotting with the indicated antibodies. Intensities of PICH signals (a.u.) normalized by β-tubulin are shown. (B) DLD-1 cells with endogenous PICH tagged with a mAID and exogenous PICH mCherry mutants were treated with auxin or auxin and doxycycline for 22 h. Mitotic chromosomes were isolated and subjected to Western blotting with the indicated antibodies. Intensities of PICH signals (a.u.) normalized by H3 are shown with mean value and SD. *p* values for comparison from three experiments were calculated using a Student's *t* test ANOVA; ns: not significant; **: $p < 0.01$. (C) WT PICH mCherry mitotic cells were fixed and stained with antibodies against SUMO2/3 (green), TopoIIα (green), and mCherry (red). DNA was stained with DAPI (blue). Scale bar = 11 μm. The mean intensities of SUMO2/3 or TopoIIα signals are shown. *p* values for comparison of all values from three experiments were calculated using a Student's *t* test; ns: not significant; **: $p < 0.01$; ***: $p < 0.001$.

overlap with SUMO2/3 foci in all K128A cells observed, regardless of treatment (Figure 8A). SUMO2/3 mean intensity was observed to significantly increase after ICRF-193 treatment (Figure 8A, left, quantification), suggesting that the response to ICRF-193 remains intact. Intriguingly, the SUMO2/3 granularity was not statistically different between control and ICRF-193–treated cells, presumably due to increased granularity caused by expression of the PICH K128A compared with PICH WT (Figure 7C). This suggests that the PICH K128A mutant interacts with SUMOylated targets but due to its inability to translocate DNA, PICH K128A remains stably associated with the chromosomes where the SUMOylated proteins are located. TopoIIα signals in PICH K128A cells showed a clear increase in intensity compared with PICH WT and more diffuse localization on chromosomes. Both total chromosomal intensity and granularity of TopoIIα showed no significant increase with ICRF-193 treatment (Figure 8A, right, quantifications). This is consistent with ΔPICH conditions (Figure 6C). This suggests that the increased chromosomal association of TopoIIα after loss of PICH is responsible for the ICRF-193 ineffectiveness in this analysis. Notably, PICH foci did not show any apparent overlap with TopoIIα foci after ICRF-193 treatment, as was observed in parental DLD-1 cells (Figure 1B) and PICH WT–replaced cells (Figure 7C). This could indicate that stable binding to other SUMO2/3-modified chromosomal proteins hinders PICH from interacting with foci-forming TopoIIα after ICRF-193 treatment. As observed by Western blot analysis, the PICH d3SIM-mCherry mutant did not show any chromosomal signal, but rather a diffuse signal was observed throughout the cell. SUMO2/3 signals were observed on chromosomes in the PICH d3SIM-expressing cells. The total intensity of SUMO2/3 signal on chromosomes was not significantly increased with ICRF-193 treatment. This might originate from the already increased level of SUMO2/3-modified proteins on chromosomes in the PICH

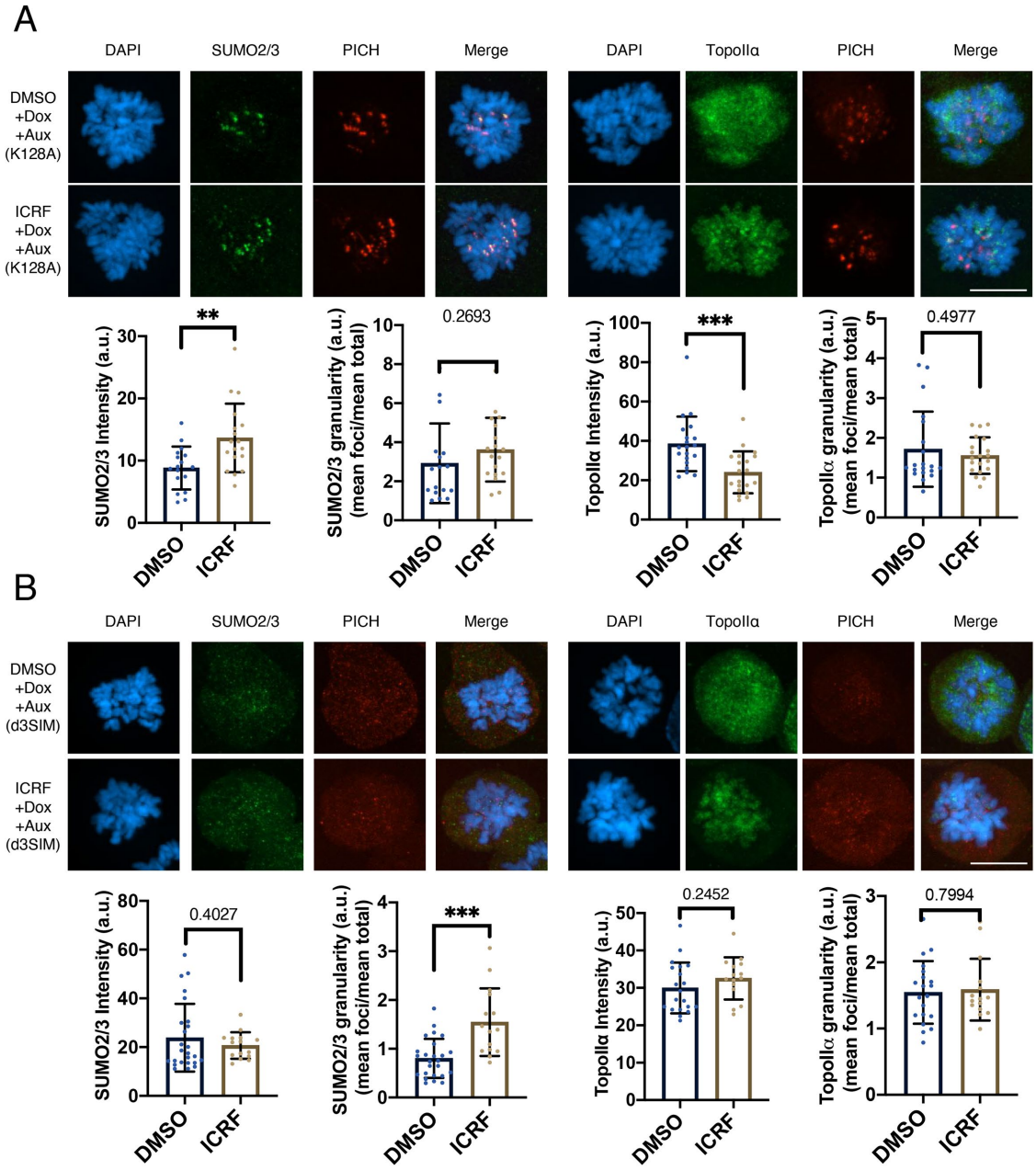

FIGURE 8: Translocase activity and SIMs on PICH are necessary for redistribution of SUMOylated proteins and SUMOylated TopoIIα on mitotic chromosomes. (A) K128A PICH mCherry mitotic cells were fixed and stained with antibodies against SUMO2/3 (green), TopoIIα (green), and mCherry (red). DNA was stained with DAPI (blue). Scale bar = 11 μm. The mean intensities of SUMO2/3 signals are shown. *p* values for comparison of all values from three experiments were calculated using a Student's *t* test ANOVA; ns: not significant; **: $p < 0.01$; ***: $p < 0.001$. (B) d3SIM PICH mCherry mitotic cells were fixed and stained with antibodies against: SUMO2/3 (green), TopoIIα (green), and mCherry (red). DNA was stained with DAPI (blue). Scale bar = 11 μm. The mean intensities of TopoIIα signals are shown. *p* values for comparison of all values from three experiments were calculated using a Student's *t* test ANOVA; ns: not significant; ***: $p < 0.001$.

d3SIM (Figure 8B, quantification) compared with PICH WT (Figure 7C). However, the granularity of SUMO2/3 showed that the ICRF-193–dependent increase of SUMO2/3 foci was retained. Similar to PICH K128A, the TopoIIα signal on the chromosome was increased compared with PICH WT, and TopoIIα localization on chromosomes in PICH d3SIM-expressing cells was more diffused. No significant difference was observed after ICRF-193 treatment in terms of total chromosomal intensity (Figure 8B, quantification). Again, consistent with ΔPICH (Figure 6C), ICRF-193 treatment did not result in an increase in TopoIIα foci formation in the PICH d3SIM-replaced cells. This suggests that the SIM-dependent chromosomal association of PICH, or regulation of SUMO2/3-modified chromosomal proteins by PICH, is required for proper distribution of TopoIIα on mitotic chromosomes. Taking the results together, using its SIMs and translocase activity, PICH attenuates the association of SUMO2/3-modified proteins with chromosomes. Thus, these activities of PICH affect chromosome organization, including TopoIIα association with chromosomes.

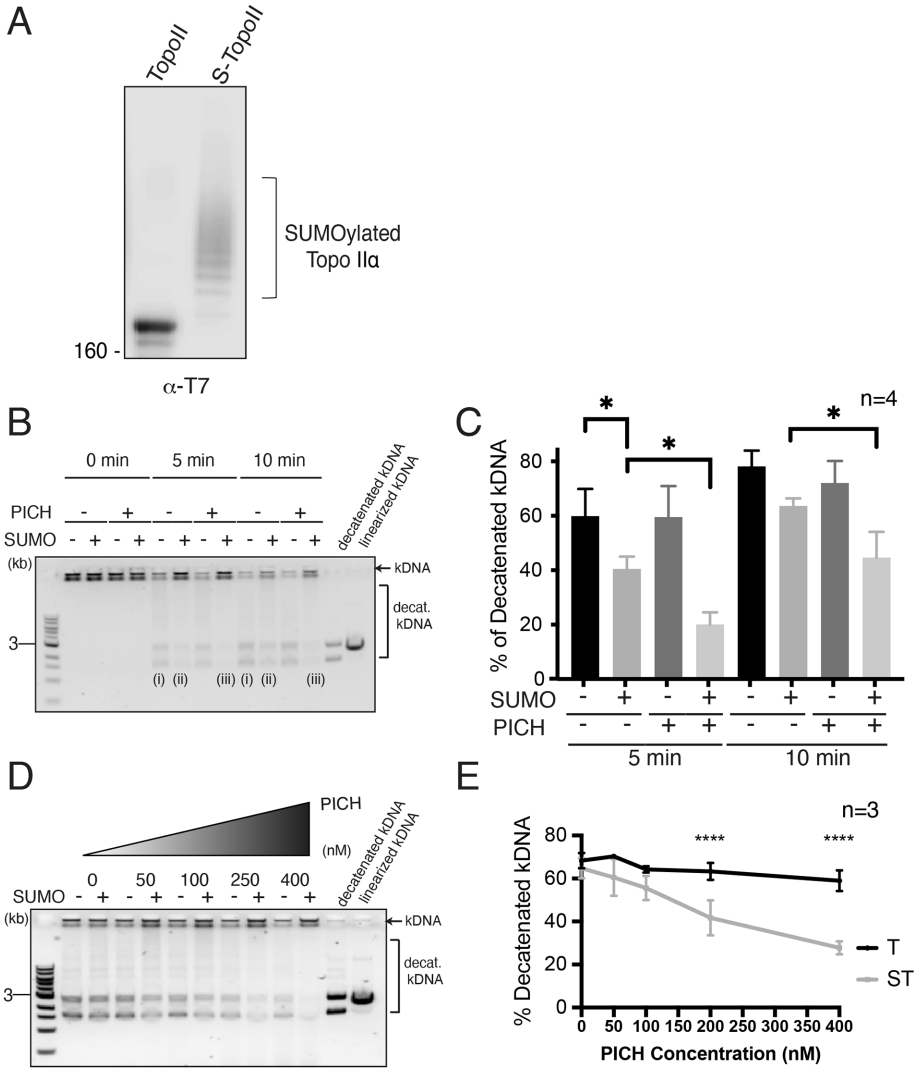

FIGURE 9: PICH inhibits SUMOylated TopoIIα decatenation activity. (A) Recombinant T7-tagged TopoIIα proteins were SUMOylated in vitro. Samples were subjected to Western blotting using anti-T7 tag antibody. The bracket indicates SUMOylated TopoIIα. (B) Representative gel after decatenation reactions with non-SUMOylated TopoIIα (–SUMO lane i) or SUMOylated TopoIIα (+ SUMO lane ii; + PICH lane iii). Catenated kDNA is indicated by an arrow. The bracket indicates the decatenated kDNA species. (C) The decatenation activity of reactions in B was calculated as a percentage of decatenated kDNA. (D) Representative gel after decatenation reactions with SUMOylated and non-SUMOylated TopoIIα with increasing concentrations of PICH. Catenated kDNA is indicated by an arrow. The bracket indicates decatenated kDNA species. (E) The decatenation activity of SUMOylated (ST) and non-SUMOylated TopoIIα (T) in D was calculated as a percentage of decatenated kDNA. Statistical analyses in C ($n = 4$) and E ($n = 3$) were performed by using a two-way ANOVA with Tukey multicomparison correction; p values for comparison among the experiments were calculated. ns: not significant; *: $p \leq 0.05$; **: $p < 0.01$; ****: $p < 0.0001$.

substrate (Ryu *et al.*, 2010b). The decatenation activity was measured by calculating the percentage of decatenated kinetoplast DNA (kDNA) separated by gel electrophoresis. On average, 70% of kDNA is decatenated at the 5- and 10-min time points when non-SUMOylated TopoIIα is present in the reaction (Figure 9B, PICH lanes marked by i). As we have previously shown, the decatenation activity of SUMOylated TopoIIα was reduced compared with non-SUMOylated TopoIIα (Figure 9B, lanes marked by ii). Importantly, when we added PICH to each of the reactions at concentrations equimolar to that of TopoIIα (200 nM), the decatenation activity of SUMOylated TopoIIα was further attenuated (Figure 9, B, marked by iii, and C). The reduction in decatenation activity of SUMOylated TopoIIα was statistically significant at both the 5- and 10-min time points (Figure 9C, light gray bars). A dose-dependent effect of PICH on SUMOylated TopoIIα decatenation activity was observed, but that was not the case for non-SUMOylated TopoIIα. The concentration of TopoIIα in the reaction was 200 nM, and PICH significantly reduced decatenation activity of SUMOylated TopoIIα ranging from 200 nM (equimolar) up to 400 nM (Figure 9, D and E). Only SUMOylated TopoIIα was inhibited by PICH dose-dependently, which is distinct from the PICH/non-SUMOylated TopoIIα interaction. PICH binding to TopoIIα has been shown to increase TopoIIα activity in vitro (Nielsen *et al.*, 2015). In our assay, however, that increase was not clearly detected. This discrepancy might originate from the assay conditions, such as the existence of SUMO in the reaction. It is possible that excess SUMO in the reaction interacts with PICH and that affects PICH interaction with unmodified TopoIIα.

To determine which activity of PICH is required for inhibiting SUMOylated TopoIIα decatenation activity, we utilized the PICH mutants that have defects in the SUMO-binding ability (PICH-d3SIM) or in translocase activity (PICH-K128A) (Figure 10A) (Sridharan and Azuma, 2016). If PICH/SUMO interaction is critical for inhibiting the decatenation activity of SUMOylated TopoIIα, the PICH-d3SIM mutant would lose its inhibitory function. In addition, we also expect that the PICH translocase activity–deficient (PICH-K128A) mutant would lose its inhibitory function on SUMOylated TopoIIα, if the translocase-deficient mutant could not remove SUMOylated TopoIIα from kDNA. Supporting our hypothesis, PICH-d3SIM lost its inhibitory function and SUMOylated TopoIIα decatenation activity returned to levels similar to that of no PICH addition (Figure 10C, compare ST to ST + PICH d3SIM). This suggests that direct SUMO/SIM interactions between PICH and SUMOylated TopoIIα have a key role in this inhibition. In contrast, the translocase-deficient PICH mutant was able to attenuate SUMOylated TopoIIα

PICH attenuates decatenation activity of SUMOylated TopoIIα dependent on its SIMs

The cell-based assays suggest that PICH is required for proper organization of chromosomal SUMOylated proteins and SUMOylated TopoIIα is one of the targets. To determine the potential role of PICH interaction with SUMOylated TopoIIα, we performed an in vitro DNA decatenation assay to compare the effect of PICH on non-SUMOylated and SUMOylated TopoIIα (Figure 9A). Using the same conditions established in our previous study, recombinant *Xenopus laevis* TopoIIα was SUMOylated in vitro, and then its DNA decatenation activity was analyzed by using catenated kDNA as the

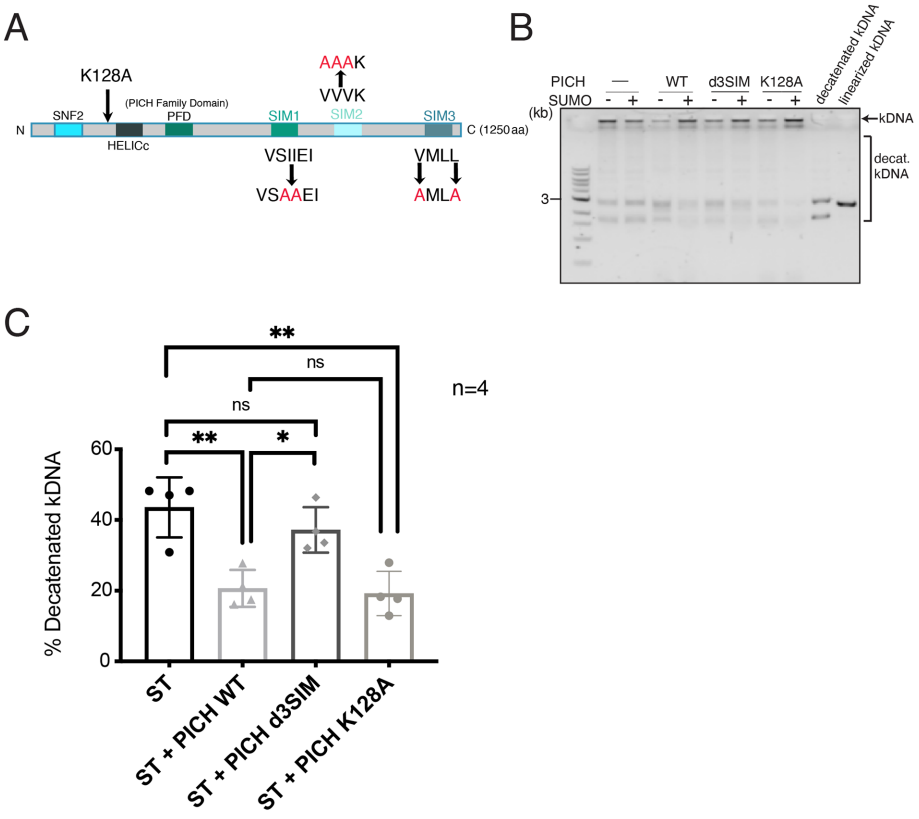

FIGURE 10: PICH SUMO-binding ability involved in suppression of SUMOylated TopoIIα decatenation activity. (A) Schematic of PICH protein with known functional motifs. The introduced mutations in SIMs and in the ATPase domain (K128A) are indicated. (B) Representative gel showing non-SUMOylated (–SUMO) and SUMOylated TopoIIα (+SUMO) activity with PICH WT, a non–SUMO-binding mutant (d3SIM), and a translocase-deficient mutant (K128A) or no PICH protein (–PICH). Catenated kDNA is indicated with an arrow. The bracket indicates decatenated kDNA species. (C) Decatenation activity of SUMOylated TopoIIα (ST) with indicated PICH (ST: no PICH, ST + PICH WT: PICH wild type, ST + PICH d3SIM: PICH-d3SIM mutant, and ST + PICH K128A: PICH-K128A mutant). Statistical analysis in C was performed by using a one-way ANOVA with Tukey multicomparison correction; *p* values for comparison among four experiments were calculated. ns: not significant; *: $p \leq 0.05$; **: $p < 0.01$.

decatenation activity, comparable to WT PICH (Figure 10C, compare ST + PICH WT and ST + PICH K128A). Notably, neither of the PICH mutants showed any apparent effect on non-SUMOylated TopoIIα (Figure 10B) compared with PICH WT. This suggests that PICH binding to DNA does not inhibit the decatenation activity of TopoIIα but rather it forms a complex with SUMOylated TopoIIα and prevents its decatenation activity. Taken together, our results suggest that PICH recognizes the SUMO moieties on TopoIIα through its SIMs to attenuate decatenation activity.

In conclusion, our results show a novel function of PICH in the organization of SUMOylated chromosomal proteins during mitosis. This activity is dependent on PICH translocase activity, and in vitro data suggest that the SUMO-interacting ability of PICH is important for the recognition of SUMOylated proteins (Figure 11).

DISCUSSION

We previously demonstrated that both DNA translocase activity and SUMO-interacting ability are required for the essential functions of PICH in proper chromosome segregation (Sridharan and Azuma, 2016). The results presented in this report provide the link between these two functions of PICH during mitosis. Collectively, the results indicate that PICH interacts with SUMOylated chromosomal proteins and regulates their distribution on mitotic chromosomes. Increasing SUMOylation, whether by a modulating deSUMOylation enzyme or using a specific inhibitor of TopoII, led to the enrichment of PICH foci on mitotic chromosomes. Mutant PICH cell lines demonstrated that both DNA translocase activity and SUMO-binding abilities of PICH are required for regulating the distribution of SUMO2/3-modified proteins on chromosomes: without these activities of PICH, increased SUMO2/3 foci formation was observed.

PICH targets and regulates chromosomal SUMOylated proteins using its SUMO-binding ability and translocase activity

SUMOylation has been shown to play a role in complex assembly by mediating SUMO/SIM interactions (Lin *et al.*, 2006; Guzzo *et al.*, 2012; Pelisch *et al.*, 2017; Matmati *et al.*, 2018). It has been demonstrated that numerous proteins are SUMOylated on mitotic chromosomes (Schimmel *et al.*, 2014; Cubenas-Potts *et al.*, 2015; Huang *et al.*, 2016). Proper regulation of SUMOylation on chromosomal proteins is apparently key to promoting faithful chromosome segregation, as revealed by modulating enzymes that control SUMOylation (Hari *et al.*, 2001; Diaz-Martinez *et al.*, 2006; Cubenas-Potts *et al.*, 2013; Pelisch *et al.*, 2014). Our current study demonstrates that SUMOylated chromosomal proteins are targeted by PICH through its SIMs. Increased SUMO2/3 modification, either by treating cells with ICRF-193 (Figure 1) or by targeting a dominant negative deSUMOylation enzyme mutant to chromosomes (Figure 4), promotes focal enrichment of PICH and SUMO2/3 on mitotic chromosomes. This suggests that PICH efficiently targets SUMOylated chromosomal proteins, including TopoIIα, and either redistributes them away from foci or evicts them from chromosomes. Given the fact that PICH can interact with SUMO moieties (Sridharan *et al.*, 2015) using its three SIMs, this enrichment of PICH foci and SUMO2/3 foci suggests that PICH can target multiple SUMOylated chromosomal proteins. More importantly, the translocase-deficient mutant of PICH showed an enrichment of SUMO2/3 and PICH foci that overlapped on chromosomes without ICRF-193 treatment (Figure 8A). This suggests that loss of translocase activity of PICH stabilizes SUMOylated protein(s) forming a stable complex on chromosomes. The PICH primary structure suggests that it acts as a nucleosome-remodeling enzyme. However, PICH has not been shown to have robust nucleosome-remodeling activity toward nucleosomes composed of canonical histones (Ke *et al.*, 2011). Our observations imply that PICH could utilize its translocase activity for remodeling chromosomal SUMOylated proteins. Because both translocase-deficient PICH and SIM-deficient PICH mutants showed defective TopoIIα localization, specifically that TopoIIα signals became diffuse and lost their response to ICRF-193 treatment (shown in Figure 8), the remodeling of SUMO2/3-modified chromosomal proteins by

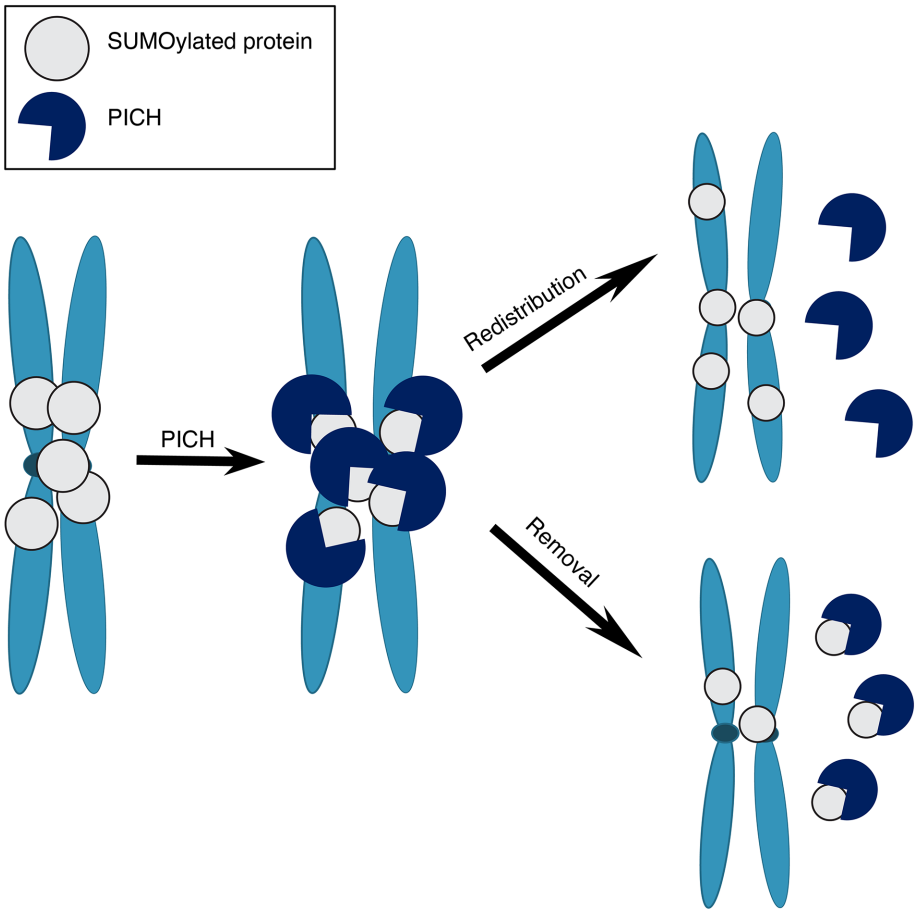

FIGURE 11: Model for demonstrating the role of PICH in regulating chromosomal SUMOylated proteins for proper chromosome segregation. SUMOylation plays a critical role in chromosome regulation and mitotic timing; this is due in part to regulating the activity and mediating the binding of critical proteins. During mitosis, proteins become SUMOylated and PICH recognizes and binds these proteins using its three SIMs and then using its translocase activity redistributes or removes SUMOylated proteins from the chromosomes, and this enables proper chromosome segregation.

PICH is required for proper organization of chromosomes. This is consistent with abnormal TopoⅡα localization on chromosomes in PICH knockdown/knockout cells, as has been shown in previous studies (Biebricher *et al.*, 2013; Nielsen *et al.*, 2015). Loss of PICH results in chromosome bridge formation in anaphase (Nielsen *et al.*, 2015), and both translocase activity and SIMs are essential for preventing chromosome bridge formation (Sridharan and Azuma, 2016). SUMOylated protein remodeling by PICH may affect the overall chromosome structure and organization. PICH-d3SIM could not localize to chromosomes, but endogenous PICH could still associate with mitotic chromosomes without TopoⅡα (Figure 5). In addition to TopoⅡα, other important chromosomal structural proteins are SUMOylated, including the SMC complex proteins (Stephan *et al.*, 2011; Wagner *et al.*, 2019; Xu and Yanagida, 2019), which are likely targets of PICH function. Therefore, chromosomal structural anomalies in PICH mutants could explain the anaphase defects described above. Alternatively, recent studies indicate that the translocase activity of PICH can be used to control the supercoiling status of DNA together with topoisomerase IIIα (TOP3A) (Bizard *et al.*, 2019). This PICH/TOP3A function could control TopoⅡα activity/binding to genomic DNA by providing the preferable DNA topology for TopoⅡα. If the SIM-deficient mutant has a defect in this PICH/TOP3A function, this DNA topology–dependent regulation of TopoⅡα could explain our results that show TopoⅡα mislocalization on chromosomes in PICH mutant–replaced cells. Further study for identification of which SUMOylated chromosomal proteins are targeted by PICH and a more detailed analysis of the chromosome structures in PICH-replaced cells will address our hypothesis.

SUMOylated TopoⅡα is a target of PICH

ICRF-193 inhibits TopoⅡα SPR by stalling TopoⅡα in a closed-clamp conformation that holds two decatenated DNA strands within TopoⅡα (Roca *et al.*, 1994; Morris *et al.*, 2000). Therefore, increased TopoⅡα foci after ICRF-193 could represent an SPR active population of TopoⅡα stalled on genomic DNA. Our results demonstrated that these stalled TopoⅡα enzymes subsequently undergo SUMOylation and are then recognized by PICH (Figures 3 and 4), mainly observed at the centromere (Figures 5 and 6). These findings provide a novel mechanistic understanding of the interaction between SUMOylated TopoⅡα and PICH and provide insight into why PICH knockout cells were found to be sensitive to ICRF-193. Perhaps more importantly, depletion of PICH led to increased abundance of TopoⅡα on mitotic chromosomes even in the absence of ICRF-193 treatment. Therefore, the data provide evidence that PICH has a specific function under physiological conditions, to regulate the abundance of TopoⅡα on chromosomes in mitosis. Though speculative, it may be the case that PICH evicts TopoⅡα that becomes stalled during the SPR even in the absence of a TopoⅡα catalytic inhibitor.

PICH can increase TopoⅡα decatenation activity in vitro, and that helps resolve tangled DNA during anaphase (Nielsen *et al.*, 2015). In addition, a recent study of PICH/TOP3A in controlling the supercoiling status of DNA for optimal TopoⅡα activity supports the specific role of PICH in controlling TopoⅡα activity on genomic DNA (Bizard *et al.*, 2019). These mechanisms certainly help TopoⅡα perform the SPR to prevent or resolve the formation of UFBs, which are created by tangled genomic DNA. In this study we presented evidence that depleting TopoⅡα abrogates the enrichment of PICH foci at centromeres even in the presence of ICRF-193 and increased SUMO2/3 foci at centromere (Figure 5), suggesting that PICH specifically targets SUMOylated TopoⅡα in ICRF-193–treated cells. Further, PICH depletion increased chromosome-associated SUMOylated TopoⅡα (Figure 6A), suggesting PICH attenuates SUMOylated TopoⅡα association with chromosomes. The SIM-dependent interaction of PICH with SUMOylated TopoⅡα was shown in the in vitro assays. PICH binding with SUMOylated TopoⅡα has different consequences, that is, inhibition of decatenation activity (Figure 9). The inhibition of activity requires SIMs, suggesting that direct interaction of PICH and SUMO moieties on TopoⅡα is critical (Figure 10). The mechanism of how both WT PICH and translocase-deficient mutants similarly inhibit the decatenation activity of SUMOylated TopoⅡα is currently unclear. If we apply our model of PICH as a

SUMOylated protein remodeler to this context, the mechanism of inhibition might be by removing SUMOylated TopoIIα from DNA. If that is the case, the translocase-deficient mutant could inhibit decatenation activity by forming a stable complex with SUMOylated TopoIIα on DNA, which can be predicted by the observation of stabilized SUMOylated protein on chromosomes in PICH-K128A–replaced cells. Further analysis of the complex formation of PICH and SUMOylated TopoIIα in vitro or in cells is our next goal in elucidating the mechanism of this inhibition.

Broader implications of the novel function of PICH as a SUMOylated protein remodeler

Our data suggest a novel function of PICH on mitotic chromosomes in remodeling SUMO2/3-modified chromosomal proteins for promoting faithful chromosome segregation. The defect in PICH SIM or translocase activity mutants causes structural abnormalities revealed by aberrant localization of TopoIIα and lack of response to ICRF-193. The remodeling activity of PICH toward SUMOylated chromosomal proteins is predicted to control their mobility on chromosomes. This can be tested by live-imaging analysis after tagging endogenous SUMO2 or 3 and visualizing localization in cells. Identification of SUMO2/3-modified proteins targeted by PICH will be critical in advancing our understanding of how temporal SUMO2/3 modification on mitotic chromosomes contributes to chromosome segregation. We expect that knowing these targets will reveal how and why loss of PICH and misregulation of mitotic SUMOylation affect chromosome structure and faithful segregation of chromosomes. One clear target of PICH is SUMOylated TopoIIα after ICRF-193 treatment. Recently, we demonstrated that ICRF-193 treatment resulted in a mitotic arrest in cells that requires SUMOylated TopoIIα and subsequent Aurora B activation (Pandey *et al.*, 2020). It is possible that PICH can control this stalled TopoIIα-dependent mitotic checkpoint by evicting SUMOylated TopoIIα from chromosomes. This can be tested using PICH depletion or replacement cell lines as well as modulating PICH activity in TopoIIα-replaced cell lines with a non-SUMOylatable mutant.

MATERIALS AND METHODS

Plasmids, constructs, and site-directed mutagenesis

The Py-S2 fusion DNA construct of human PIASy-NTD (amino acids 1–135) and SENP2-CD (amino acids 363–589) was created by the fusion PCR method using a Glycine-Alanine linker between the two fragments. Then the Py-S2 fusion DNA fragment was subcloned into a recombinant expression pET28a plasmid at the *Bam*HI/*Xho*I sites. To generate the Py-S2 Mut fusion DNA construct, substitution of cysteine to alanine at 548 in Py-S2 was introduced using a site-directed mutagenesis QuikChangeII kit (Agilent) by following the manufacturer's instructions. hH11 locus and CCR5 locus targeting donor plasmids for inducible expression of Py-S2 proteins were created by modifying the pMK243 (Tet-OsTIR1-PURO) plasmid (Natsume *et al.*, 2016). pMK243 (Tet-OsTIR1-PURO) was purchased from Addgene (#72835), and the OsTIR1 fragment was removed by *Bgl*II and *Mlu*I digestion, followed by an insertion of a multicloning site. Homology arms for each locus were amplified from DLD-1 genomic DNA using the primers listed in the Supplemental Information. The Py-S2 fused with mNeon cDNA and PICH-mCherry–fused cDNA were inserted at the *Mlu*I and *Sal*I sites of the modified pMK243 plasmid. For the CCR5 targeting plasmid, the antibiotics-resistant gene was changed to zeocin-resistant from puromycin-resistant. The original plasmid for OsTIR1 targeting to the RCC1 locus was created by inserting the TIR1 sequence amplified from the pBABE TIR1-9Myc (Addgene #47328; Holland *et al.*, 2012) plasmid, the blasticidin-resistant gene (BSD) amplified from pQCXIB with ires-blast (Takara/Clontech), and miRFP670 amplified from the pmiRFP670-N1 plasmid (Addgene #79987; Shcherbakova *et al.*, 2016) into the pEGFP-N1 vector (Takara/Clontech) with homology arms for the RCC1 C-terminal locus. Using genomic DNA obtained from a DLD-1 cell as a template DNA, the homology arms were amplified using primers listed in the Supplemental Information. Further, the OsTIR1 targeting plasmid was modified by eliminating the miRFP670 sequence by PCR amplification of the left homology arm and the TIR/BSD/right homology arm for inserting into pMK292 obtained from Addgene (#72830) (Natsume *et al.*, 2016) using *Xma*I/*Bst*BI sites. Three copies of codon-optimized micro AID tag (50 amino acids each; Morawska and Ulrich, 2013) were synthesized by the IDT Company, and the hygromycin-resistant gene/P2A sequence was inserted upstream of the 3x micro AID sequence. The 3xFlag sequence from the p3xFLAG-CMV-7.1 plasmid (Sigma) was inserted downstream of the AID sequence. The homology arms sequences for PICH N-terminal insertion and TopoIIα N-terminal insertion were amplified using primers listed in the Supplemental Information from genomic DNA of a DLD-1 cell and then inserted into the plasmid by using *Pci*I/*Sal*I and *Spe*I/*Not*I sites. In all of the RCC1 locus, PICH locus, TopoIIα locus, CCR5 locus, and hH11 locus genome-editing cases, the guide RNA sequences listed in the Supplemental Information were designed using CRISPR Design Tools from https://figshare.com/articles/CRISPR_Design_Tool/1117899 (Rafael Casellas laboratory, National Institutes of Health) and (Zhang laboratory, MIT) inserted into pX330 (Addgene #42230). Mutations were introduced in PAM sequences on the homology arms. The *X. laevis* TopoIIα cDNA and human PICH cDNA were subcloned into a pPIC 3.5K vector in which calmodulin-binding protein CBP-T7 tag sequences were inserted as previously described (Ryu *et al.*, 2010b; Sridharan and Azuma, 2016). All mutations in the plasmids were generated by site-directed mutagenesis using a QuikChangeII kit (Agilent) according to the manufacturer's instructions. All constructs were verified by DNA sequencing.

Recombinant protein expression and purification, and preparation of antibodies

Recombinant TopoIIα and PICH proteins were prepared as previously described (Ryu *et al.*, 2010b; Sridharan and Azuma, 2016). In brief, the pPIC 3.5K plasmids carrying TopoIIα or PICH cDNA fused with calmodulin-binding protein-tag were transformed into the GS115 strain of *Pichia pastoris* yeast and expressed by following the manufacturer's instructions (Thermo/Fisher). Yeast cells expressing recombinant proteins were frozen and ground with a coffee grinder that contains dry ice, suspended with lysis buffer (50 mM Tris-HCl, pH 7.5, 150 mM NaCl, 2 mM $CaCl_2$, 1 mM $MgCl_2$, 0.1% Triton X-100, 5% glycerol, 1 mM dithiothreitol [DTT], complete EDTA-free Protease inhibitor tablet [Roche], and 10 mM phenylmethylsulfonyl fluoride). The lysed samples were centrifuged at 25,000 × *g* for 40 min. To capture the CBP-tagged proteins, the supernatant was mixed with calmodulin-Sepharose resin (GE Healthcare) for 90 min at 4°C. The resin was then washed with lysis buffer, and proteins were eluted with buffer containing 10 mM ethylene glycol-bis(β-aminoethyl ether)-*N*,*N*,*N*′,*N*′-tetraacetic acid. In the case of PICH, the elution was concentrated by centrifugal concentrator (Amicon ultra with a 100-kDa-molecular-weight cutoff). In the case of TopoIIα, the elution was further purified by Hi-trap Q anion-exchange chromatography (GE Healthcare). Recombinant Py-S2 proteins fused to the hexa-histidine tag were expressed in Rossetta2 (DE3) (EMD Millipore/Novagen) and purified with hexa-histidine affinity resin (Talon beads from Takara/Clontech). Fractions by imidazole-elution

were subjected to Hi-trap SP cation-exchange chromatography. The peak fractions were pooled and then concentrated by centrifugal concentrator (Amicon ultra with a 30-kDa-molecular-weight cutoff). The E1 complex (Aos1/Uba2 heterodimer), PIASy, Ubc9, dnUbc9, and SUMO paralogues were expressed in Rosetta2(DE3) and purified as described previously (Ryu *et al*., 2010a).

To generate the antibody for human PICH, the 3′end (coding for amino acids 947–1250) was amplified from PICH cDNA by PCR. The amplified fragment was subcloned into the pET28a vector (EMD Millipore/Novagen), and then the sequence was verified by DNA sequencing. The recombinant protein was expressed in Rossetta2(DE3) strain (EMD Millipore/Novagen). Expressed protein was found in the inclusion body; thus the proteins were solubilized by 8 M urea-containing buffer (20 mM HEPES, pH 7.8, 300 mM NaCl, 1 mM $MgCl_2$, 0.5 mM tris(2-carboxyethyl)phosphine). The solubilized protein was purified by Talon-resin (Clontech/Takara) using the hexa-histidine-tag fused at the N-terminus of the protein. The purified protein was separated by SDS–PAGE, and protein was excised after Instant*Blue* (Sigma-Aldrich) staining. The gel slice was used as an antigen, and immunization of rabbits was done by Pacific Immunology, USA. To generate the primary antibody for human TopoIIα, the 3′end of TopoIIα (coding for amino acids 1359–1589) was amplified from TopoIIα cDNA by PCR. The amplified fragment was subcloned into pET28a and pGEX-4T vectors (GE Healthcare), and then the sequence was verified by DNA sequencing. The recombinant protein was expressed in Rossetta2(DE3). The expressed protein was purified using hexa-histidine-tag and GST-tag by Talon-resin (Clontech/Takara) or glutathione-Sepharose (GE Healthcare) following the manufacturer's protocol. The purified proteins were further separated by cation-exchange column. Purified hexa-histidine-tagged TopoIIα protein as used as an antigen, and immunization of rabbits was done by Pacific Immunology, USA. For both PICH and TopoIIα antigens, antigen affinity columns were prepared by conjugating purified antigens (hexa-histidine-tagged PICH C-terminus fragment or GST-tagged TopoIIα C-terminus fragment) to the NHS(N-hydroxysuccinimide)-activated Sepharose resin following the manufacturer's protocol (GE Healthcare). The rabbit antisera were subjected to affinity purification using antigen affinity columns. Secondary antibodies used for this study and their dilution rates were, for Western blotting, goat anti-rabbit (IRDye 680RD, 1/20,000, LI-COR) and goat anti-mouse (IRDye 800CW, 1/20,000, LI-COR), and for immunofluorescence staining, goat anti-mouse immunoglobulin G [IgG] Alexa Fluor 568 (#A11031, 1:500, Invitrogen), goat anti-rabbit IgG Alexa Fluor 568 (#A11036, 1:500, Thermo/Fisher), goat anti-rabbit IgG Alexa Fluor 488 (#A11034, 1:500, Thermo/Fisher), and goat anti-guinea pig IgG Alexa Fluor 568 (#A21450, 1:500, Thermo/Fisher). Unless otherwise stated, all chemicals were obtained from Sigma-Aldrich.

In vitro SUMOylation assays and decatenation assays

The SUMOylation reactions were performed in the reaction buffer (20 mM HEPES, pH 7.8, 100 mM NaCl, 5 mM $MgCl_2$, 0.05% Tween 20, 5% glycerol, 2.5 mM ATP, and 1 mM DTT) by adding 15 nM E1, 15 nM Ubc9, 45 nM PIASy, 500 nM T7-tagged TopoIIα, and 5 μM SUMO2-GG. For the non-SUMOylated TopoIIα control, 5 μM SUMO2-G mutant was used instead of SUMO2-GG. After the reaction with the incubation for 1 h at 25°C, it was stopped with the addition of EDTA at a final concentration of 10 mM. For the analysis of the SUMOylation profile of TopoIIα 3X SDS–PAGE sample buffer was added to the reaction, and the samples were resolved on 8–16% Tris-HCl gradient gels (#XP08165BOX, Thermo/Fisher) by SDS–PAGE and then analyzed by Western blotting with horseradish peroxidase–conjugated anti-T7 monoclonal antibody (#T3699, EMD Millipore/Novagen).

Decatenation assays were performed in the decatenation buffer (50 mM Tris-HCl, pH 8.0, 120 mM NaCl, 5 mM $MgCl_2$, 0.5 mM DTT, 30 μg bovine serum albumin [BSA]/ml, and 2 mM ATP) with SUMOylated TopoIIα and non-SUMOylated TopoIIαn and with 6.2 ng/μl of kDNA (TopoGEN). The resction was performed at 25°C with the conditions indicated in each of the figures. The reactions were stopped by adding one-third volume of 6X DNA dye (30% glycerol, 0.1% SDS, 10 mM EDTA, and 0.2 μg/μl bromophenol blue). The samples were loaded on a 1% agarose gel containing SYBR Safe DNA Gel stain (#S33102, Invitrogen) with 1 kb ladder (#N3232S, NEB) and electrophoresed at 100 V in TAE buffer (Tris-acetate-EDTA) until the marker dye reached the middle of the gel. The amount of kDNA remaining in the wells was measured using ImageStudio, and the percentage of decatenated DNA was calculated as (intensity of initial kDNA [at 0 min incubation] – intensity of remaining catenated DNA)/intensity of initial kDNA. Obtained percentages of catenated DNA were plotted and analyzed for the statistics by using GraphPad Prism 8 Software.

Cell culture, transfection, and colony isolation

Targeted insertion using the CRISPR/Cas9 system was used for all integration of exogenous sequences into the genome. DLD-1 cells were transfected with guide plasmids and donor plasmid using ViaFect (#E4981, Promega) on 3.5 cm dishes. The cells were split and replated on 10 cm dishes at ~20% confluency; 2 d later, the cells were subjected to a selection process by being maintained in the medium in the presence of a desired selection reagent (1 μg/ml blasticidin [#ant-bl, Invivogen], 400 μg/ml zeocin [#ant-zn, Invivogen], 200 μg/ml hygromycin B gold [#ant-hg, Invivogen]). The cells were cultured for 10–14 d with a selection medium, the colonies were isolated and grown in 48-well plates, and Western blotting and genomic DNA samples were prepared to verify the insertion of the transgene. Specifically, for the Western blotting analysis, the cells were pelleted and 1X SDS–PAGE sample buffer was added and boiled/vortexed. Samples were separated on an 8–16% gel and then blocked with casein and probed using the antibody described in each figure legend. Signals were acquired using the LI-COR Odyssey Fc imager. To perform genomic PCR, the cells were pelleted, and genomic DNA was extracted using lysis buffer (100 mM Tris-HCl, pH 8.0, 200 mM NaCl, 5 mM EDTA, 1% SDS, and 0.6 mg/ml proteinase K [#P8107S, NEB]) and purified by ethanol precipitation followed by resuspension with TE buffer containing 50 μg/ml RNase A (#EN0531,ThermoFisher). Primers used for confirming the proper integrations are listed in the Supplemental Information.

To establish AID cell lines, as an initial step, the *Oryza sativa* E3 ligase (OsTIR1) gene was inserted into the 3′ end of a housekeeping gene, RCC1, using the CRISPR/Cas9 system in the DLD-1 cell line. The RCC1 locus was an appropriate locus to accomplish the modest but sufficient expression level of the OsTIR1 protein so that it would not induce a nonspecific degradation without the addition of auxin (Supplemental Figure S3) (Yau *et al*., 2020). We then introduced DNA coding for AID-3xFlag tag into the TopoIIα or PICH locus using CRISPR/Cas9 editing into the OsTIR1-expressing parental line (Supplemental Figures S4 and S5). The isolated candidate clones were subjected to genomic PCR and Western blotting analysis to validate integration of the transgene. Once clones were established and the transgene integration was validated, the depletion of the protein in the auxin-treated cells was confirmed by Western blotting and immunostaining.

Introducing DNA encoding Tet-inducible PICH mCherry into the CCR5 locus or inducible Py-S2 into hH11 was done by CRISPR/Cas9 editing into the desired locus (Supplemental Figures S2 and S6). The OsTIR1-expressing mAID PICH parental cell line was used for introduction of the PICH mCherry mutants targeted to the CCR5 locus. The isolated candidate clones were subjected to genomic PCR and Western blotting analysis to validate integration of the transgene. Once clones were established and the transgene integration was validated, the expression of the transgenes was confirmed by the addition of doxycycline.

Xenopus egg extract assay for mitotic chromosomal SUMOylation analysis

Low-speed cytostatic factor (CSF)-arrested XEEs and demembraned sperm nuclei were prepared following standard protocols (Murray, 1991; Powers *et al.*, 2001). To prepare the mitotic replicated chromosome, CSF extracts were driven into interphase by adding 0.6 mM $CaCl_2$. Demembraned sperm nuclei were added to interphase extract at 4000 sperm nuclei/μl and then incubated for ~60 min to complete DNA replication confirmed by the morphology of nuclei. Then an equal volume of CSF XEE was added to the reactions to induce mitosis. To confirm the activities of Py-S2 proteins on mitotic SUMOylation, the Py-S2 proteins or dnUbC9 were added to XEEs at final concentrations of 30 nM or 5 μM, respectively, at the onset of mitosis induction. After mitotic chromosome formation was confirmed by microscopic analysis of condensed mitotic chromosomes, chromosomes were isolated by centrifugation using a 40% glycerol cushion as previously described (Yoshida *et al.*, 2016), and then the isolated mitotic chromosomes were boiled in SDS–PAGE sample buffer. Samples were resolved on 8–16% gradient gels and subjected to Western blotting with the indicated antibodies. Signals were acquired using a LI-COR Odyssey Fc digital imager, and the quantification was performed using Image Studio Lite software.

The following primary antibodies were used for Western blotting: rabbit anti-*Xenopus* TopoIIα (1:10,000), rabbit anti-*Xenopus* PARP1 (1:10,000), rabbit anti-SUMO2/3 (1:1000) (all prepared as described previously [Ryu *et al.*, 2010a]), anti-histone H3 (#14269, Cell Signaling).

Preparation of mitotic cells and chromosome isolation

DLD-1 cells were grown in McCoy's 5A 1x L-glutamine 10% fetal bovine serum (FBS) media for no more than 10 passages. To analyze mitotic chromosomes, cells were synchronized by the thymidine/nocodazole cell cycle arrest protocol. In brief, cells were arrested with 2 mM thymidine for 17 h, released from the thymidine block by three washes with non-FBS–containing McCoy's 5A 1x L-glutamine media, and placed in fresh 10% FBS-containing media. Six hours after the thymidine release, 0.1 μg/ml nocodazole was added to the cells for 4 additional hours and mitotic cells were isolated by performing a mitotic shake off and washed three times using McCoy's non-FBS–containing media for release from nocodazole. The cells were then resuspended with 10% FBS-containing fresh media and 7 μM of ICRF-193, 40 μM merbarone, or an equal volume of DMSO, plated on fibronectin-coated cover slips, and incubated for 20 min (NEUVITRO, #GG-12-1.5-Fibronectin). To isolate mitotic chromosomes, the cells were lysed with lysis buffer (250 mM sucrose, 20 mM HEPES, 100 mM NaCl, 1.5 mM $MgCl_2$, 1 mM EDTA, 1 mM EGTA, 0.2% Triton X-100, 1:2000 LPC [leupeptin, pepstatin, chymostatin; 20 mg each/ml in DMSO; Sigma-Aldrich], and 20 mM iodoacetamide [Sigma-Aldrich #I1149]) and incubated for 5 min on ice. Lysed cells were then placed on a 40% glycerol containing 0.25% Triton X-100 cushion and spun at 10,000 × *g* for 5 min twice. Isolated chromosomes were then boiled with SDS–PAGE sample buffer, resolved on an 8–16% gradient gel, and subjected to Western blotting with the indicated antibodies. Signals of the blotting were acquired using the LI-COR Odyssey Fc machine.

The following primary antibodies were used for Western blotting: rabbit anti-PICH (1:1000) and rabbit anti-TopoIIα (1:20,000) (both prepared as described above), rabbit anti-SUMO2/3 (1:1000), rabbit anti-histone H2A (1:2000) (#18255, Abcam), rabbit anti-histone H3 (1:2000) (#14269, Cell Signaling), rabbit anti-PIASy (1:500) (as described in Azuma *et al.*, 2005), mouse anti–β-actin (1:2000) (#A2228, Sigma-Aldrich), mouse anti-myc (1:1000) (#9E10, Santa Cruz), mouse anti–β-tubulin (1:2000) (#T4026, Sigma-Aldrich), and mouse anti-Flag (1:1000) (#F1804, Sigma-Aldrich).

Cell fixation and staining

To fix the mitotic cells on fibronectin-coated cover slips, cells were incubated with 4% paraformaldehyde (PFA) for 10 min at room temperature and subsequently washed three times with 1X phosphate-buffered saline (PBS) containing 10 mM Tris-HCl to quench PFA. Following the fixation, the cells were permeabilized using 100% ice cold methanol in a –20°C freezer for 5 min. Cells were then blocked using 2.5% hydrolyzed gelatin for 30 min at room temperature. Following blocking, the cells were stained with primary antibodies for 1 h at room temperature, washed three times with 1X PBS containing 0.1% Tween 20, and incubated with secondary antibodies for 1 h at room temperature. Following secondary incubation, cells were washed three times with 1X PBS-Tween20 and mounted onto slide glass using VECTASHIELD Antifade Mounting Medium with 4′,6-diamidino-2-phenylindole (#H-1200, Vector Laboratory) and sealed with nail polish. Images were acquired using an UltraView VoX spinning-disk confocal system (PerkinElmer) mounted on an Olympus IX71 inverted microscope. It was equipped with a software-controlled piezoelectric stage for rapid *Z*-axis movement. Images were collected using a 60 × 1.42 NA planapochromatic objective (Olympus) and an ORCA ERAG camera (Hamamatsu Photonics). Solid state 405-, 488-, and 561-nm lasers were used for excitation. Fluorochrome-specific emission filters were used to prevent emission bleed through between fluorochromes. This system was controlled by Volocity software (PerkinElmer). Minimum- and maximum-intensity cutoffs (black and white levels) for each channel were chosen in Volocity before images were exported. Images are presented as extended focus. No other adjustments were made to the images. The cell images of Supplemental figures were acquired using the Plan Apo 100x/1.4 objective lens on a Nikon Ti Eclipse microscope-equipped Exi Aqua CCD camera (Q Imaging) or a Nikon TE2000-UVequipped PRIME-BSI CMOS camera (Photometrics) with MetaMorph imaging software. Figures were prepared from exported images in Adobe illustrator.

The following primary antibodies were used for staining: rabbit anti-PICH 1:800 and rabbit anti-human TopoIIα 1:1000 (bothprepared as described above), mouse anti-human TopoIIα 1:300 (#Ab 189342, Abcam), mouse anti-SUMO2/3 (#12F3, Cytoskeleton), guinea pig anti-SUMO2/3 (1:300) (prepared as previously described [Ryu *et al.*, 2010a]), and rat anti-RFP (#RMA5F8, Bulldog Bio).

Statistical analysis of immunofluorescence images

Quantification was performed by measuring at least five chromosomes per treatment across three individual experiments. This was done by outlining the chromosome and superimposing that drawing onto the other channels before measuring. All data provided are mean intensities. PICH foci intensity were measured in Figure 1

by creating a 10-pixel-diameter circle on chromosome ends, superimposing circles onto PICH channels, and measuring mean intensities. The granularity measurements were performed using a 10-pixel-diameter circle to select foci to measure the intensity of foci. The mean foci intensity was then divided by the mean intensity of the total chromosomal signal measured by outlining chromosomes as described above. Individual chromosomes form five cells/treatment across three individual experiments were measured to obtain at lease 20 data points. Mean plus SD are plotted on all graphs.

Statistical analysis

All statistical analyses were performed with either one- or two-way analysis of variance (ANOVA), followed by the appropriate post-hoc analyses using GraphPad Prism 8 software. Graphs are presented as mean with SD.

Animal use

For the XEE assay, frog eggs were collected from a mature female *X. laevis*, and sperm was obtained from matured male *X. laevis*. The animal use protocol for the *X. laevis* studies was approved by the University of Kansas Institutional Animal Care and Use Committee.

ACKNOWLEDGMENTS

We thank M. Azuma, V. Paolillo, and B. R. Oakley at the University of Kansas for the use of their microscopes and for technical assistance during microscope and software usage. We also thank D. Clarke at the University Minnesota and Y. Yamashita at the University of Michigan for the critical reading of the manuscript and comments on this project. This work was supported by National Institutes of Health/National Institute of General Medical Sciences GM112893 and, in part, by a University of Kansas Cancer Center/Cancer Biology pilot grant (KAN1000623). The establishment of the AID-mediated knockdown system was supported by V. A., A. A., and M. D., who are supported by the National Institute of Child Health and Human Development Intramural projects Z01 HD008954 and ZIA HD001902.

REFERENCES

Agostinho M, Santos V, Ferreira F, Costa R, Cardoso J, Pinheiro I, Rino J, Jaffray E, Hay RT, Ferreira J (2008). Conjugation of human topoisomerase 2 alpha with small ubiquitin-like modifiers 2/3 in response to topoisomerase inhibitors: cell cycle stage and chromosome domain specificity. Cancer Res 68, 2409–2418.

Azuma Y, Arnaoutov A, Anan T, Dasso M (2005). PIASy mediates SUMO-2 conjugation of topoisomerase-II on mitotic chromosomes. EMBO J 24, 2172–2182.

Bachant J, Alcasabas A, Blat Y, Kleckner N, Elledge SJ (2002). The SUMO-1 isopeptidase Smt4 is linked to centromeric cohesion through SUMO-1 modification of DNA topoisomerase II. Mol Cell 9, 1169–1182.

Bauer DL, Marie R, Rasmussen KH, Kristensen A, Mir KU (2012). DNA catenation maintains structure of human metaphase chromosomes. Nucleic Acids Res 40, 11428–11434.

Baumann C, Korner R, Hofmann K, Nigg EA (2007). PICH, a centromere-associated SNF2 family ATPase, is regulated by Plk1 and required for the spindle checkpoint. Cell 128, 101–114.

Biebricher A, Hirano S, Enzlin JH, Wiechens N, Streicher WW, Huttner D, Wang LH, Nigg EA, Owen-Hughes T, Liu Y, *et al.* (2013). PICH: a DNA translocase specially adapted for processing anaphase bridge DNA. Mol Cell 51, 691–701.

Bizard AH, Allemand JF, Hassenkam T, Paramasivam M, Sarlos K, Singh MI, Hickson ID (2019). PICH and TOP3A cooperate to induce positive DNA supercoiling. Nat Struct Mol Biol 26, 267–274.

Chan KL, North PS, Hickson ID (2007). BLM is required for faithful chromosome segregation and its localization defines a class of ultrafine anaphase bridges. EMBO J 26, 3397–3409.

Cubenas-Potts C, Goeres JD, Matunis MJ (2013). SENP1 and SENP2 affect spatial and temporal control of sumoylation in mitosis. Mol Biol Cell 24, 3483–3495.

Cubenas-Potts C, Srikumar T, Lee C, Osula O, Subramonian D, Zhang XD, Cotter RJ, Raught B, Matunis MJ (2015). Identification of SUMO-2/3-modified proteins associated with mitotic chromosomes. Proteomics 15, 763–772.

Diaz-Martinez LA, Gimenez-Abian JF, Azuma Y, Guacci V, Gimenez-Martin G, Lanier LM, Clarke DJ (2006). PIASgamma is required for faithful chromosome segregation in human cells. PLoS One 1, e53.

Gomez R, Viera A, Berenguer I, Llano E, Pendas AM, Barbero JL, Kikuchi A, Suja JA (2014). Cohesin removal precedes topoisomerase IIalpha-dependent decatenation at centromeres in male mammalian meiosis II. Chromosoma 123, 129–146.

Guzzo CM, Berndsen CE, Zhu J, Gupta V, Datta A, Greenberg RA, Wolberger C, Matunis MJ (2012). RNF4-dependent hybrid SUMO-ubiquitin chains are signals for RAP80 and thereby mediate the recruitment of BRCA1 to sites of DNA damage. Sci Signal 5, ra88.

Hari KL, Cook KR, Karpen GH (2001). The Drosophila Su(var)2–10 locus regulates chromosome structure and function and encodes a member of the PIAS protein family. Genes Dev 15, 1334–1348.

Hengeveld RC, de Boer HR, Schoonen PM, de Vries EG, Lens SM, van Vugt MA (2015). Rif1 is required for resolution of ultrafine DNA bridges in anaphase to ensure genomic stability. Dev Cell 34, 466–474.

Holland AJ, Fachinetti D, Han JS, Cleveland DW (2012). Inducible, reversible system for the rapid and complete degradation of proteins in mammalian cells. Proc Natl Acad Sci USA 109, E3350–E3357.

Huang C, Cheng J, Bawa-Khalfe T, Yao X, Chin YE, Yeh ETH (2016). SUMOylated ORC2 recruits a histone demethylase to regulate centromeric histone modification and genomic stability. Cell Rep 15, 147–157.

Ke Y, Huh JW, Warrington R, Li B, Wu N, Leng M, Zhang J, Ball HL, Li B, Yu H (2011). PICH and BLM limit histone association with anaphase centromeric DNA threads and promote their resolution. EMBO J 30, 3309–3321.

Kurasawa Y, Yu-Lee LY (2010). PICH and cotargeted Plk1 coordinately maintain prometaphase chromosome arm architecture. Mol Biol Cell 21, 1188–1199.

Lin DY, Huang YS, Jeng JC, Kuo HY, Chang CC, Chao TT, Ho CC, Chen YC, Lin TP, Fang HI, *et al.* (2006). Role of SUMO-interacting motif in Daxx SUMO modification, subnuclear localization, and repression of sumoylated transcription factors. Mol Cell 24, 341–354.

Losada A, Hirano M, Hirano T (1998). Identification of Xenopus SMC protein complexes required for sister chromatid cohesion. Genes Dev 12, 1986–1997.

Matmati S, Vaurs M, Escandell JM, Maestroni L, Nakamura TM, Ferreira MG, Geli V, Coulon S (2018). The fission yeast Stn1-Ten1 complex limits telomerase activity via its SUMO-interacting motif and promotes telomeres replication. Sci Adv 4, eaar2740.

Michaelis C, Ciosk R, Nasmyth K (1997). Cohesins: chromosomal proteins that prevent premature separation of sister chromatids. Cell 91, 35–45.

Morales C, Losada A (2018). Establishing and dissolving cohesion during the vertebrate cell cycle. Curr Opin Cell Biol 52, 51–57.

Morawska M, Ulrich HD (2013). An expanded tool kit for the auxin-inducible degron system in budding yeast. Yeast 30, 341–351.

Morris SK, Baird CL, Lindsley JE (2000). Steady-state and rapid kinetic analysis of topoisomerase II trapped as the closed-clamp intermediate by ICRF-193. J Biol Chem 275, 2613–2618.

Murray AW (1991). Cell cycle extracts. Methods Cell Biol 36, 581–605.

Nacerddine K, Lehembre F, Bhaumik M, Artus J, Cohen-Tannoudji M, Babinet C, Pandolfi PP, Dejean A (2005). The SUMO pathway is essential for nuclear integrity and chromosome segregation in mice. Dev Cell 9, 769–779.

Natsume T, Kiyomitsu T, Saga Y, Kanemaki MT (2016). Rapid protein depletion in human cells by auxin-inducible degron tagging with short homology donors. Cell Rep 15, 210–218.

Nielsen CF, Huttner D, Bizard AH, Hirano S, Li TN, Palmai-Pallag T, Bjergregaard VA, Liu Y, Nigg EA, Wang LH, Hickson ID (2015). PICH promotes sister chromatid disjunction and co-operates with topoisomerase II in mitosis. Nat Commun 6, 8962.

Nishimura K, Fukagawa T, Takisawa H, Kakimoto T, Kanemaki M (2009). An auxin-based degron system for the rapid depletion of proteins in nonplant cells. Nat Methods 6, 917–922.

Ohkuni K, Levy-Myers R, Warren J, Au WC, Takahashi Y, Baker RE, Basrai MA (2018). N-terminal sumoylation of centromeric histone H3 variant

Cse4 regulates its proteolysis to prevent mislocalization to non-centromeric chromatin. G3 (Bethesda) 8, 1215–1223.
Pandey N, Keifenheim D, Yoshida MM, Hassebroek VA, Soroka C, Azuma Y, Clarke DJ (2020). Topoisomerase II SUMOylation activates a metaphase checkpoint via Haspin and Aurora B kinases. J Cell Biol 219, e201807189.
Papapetrou EP, Schambach A (2016). Gene insertion into genomic safe harbors for human gene therapy. Mol Ther 24, 678–684.
Patel S, Jazrawi E, Creighton AM, Austin CA, Fisher LM (2000). Probing the interaction of the cytotoxic bisdioxopiperazine ICRF-193 with the closed enzyme clamp of human topoisomerase IIalpha. Mol Pharmacol 58, 560–568.
Pelisch F, Sonneville R, Pourkarimi E, Agostinho A, Blow JJ, Gartner A, Hay RT (2014). Dynamic SUMO modification regulates mitotic chromosome assembly and cell cycle progression in Caenorhabditis elegans. Nat Commun 5, 5485.
Pelisch F, Tammsalu T, Wang B, Jaffray EG, Gartner A, Hay RT (2017). A SUMO-dependent protein network regulates chromosome congression during oocyte meiosis. Mol Cell 65, 66–77.
Powers M, Evans EK, Yang J, Kornbluth S (2001). Preparation and use of interphase Xenopus egg extracts. Curr Protoc Cell Biol Chapter 11, Unit 11.10.
Reverter D, Lima CD (2004). A basis for SUMO protease specificity provided by analysis of human Senp2 and a Senp2-SUMO complex. Structure 12, 1519–1531.
Reverter D, Lima CD (2006). Structural basis for SENP2 protease interactions with SUMO precursors and conjugated substrates. Nat Struct Mol Biol 13, 1060–1068.
Roca J, Ishida R, Berger JM, Andoh T, Wang JC (1994). Antitumor bisdioxopiperazines inhibit yeast DNA topoisomerase II by trapping the enzyme in the form of a closed protein clamp. Proc Natl Acad Sci USA 91, 1781–1785.
Ruan J, Li H, Xu K, Wu T, Wei J, Zhou R, Liu Z, Mu Y, Yang S, Ouyang H, *et al.* (2015). Highly efficient CRISPR/Cas9-mediated transgene knockin at the H11 locus in pigs. Sci Rep 5, 14253.
Ryu H, Al-Ani G, Deckert K, Kirkpatrick D, Gygi SP, Dasso M, Azuma Y (2010a). PIASy mediates SUMO-2/3 conjugation of poly(ADP-ribose) polymerase 1 (PARP1) on mitotic chromosomes. J Biol Chem 285, 14415–14423.
Ryu H, Azuma Y (2010). Rod/Zw10 complex is required for PIASy-dependent centromeric SUMOylation. J Biol Chem 285, 32576–32585.
Ryu H, Furuta M, Kirkpatrick D, Gygi SP, Azuma Y (2010b). PIASy-dependent SUMOylation regulates DNA topoisomerase IIalpha activity. J Cell Biol 191, 783–794.
Ryu H, Yoshida MM, Sridharan V, Kumagai A, Dunphy WG, Dasso M, Azuma Y (2015). SUMOylation of the C-terminal domain of DNA topoisomerase IIalpha regulates the centromeric localization of claspin. Cell Cycle 14, 2777–2784.
Schimmel J, Eifler K, Sigurethsson JO, Cuijpers SA, Hendriks IA, Verlaan-de Vries M, Kelstrup CD, Francavilla C, Medema RH, Olsen JV, Vertegaal AC (2014). Uncovering SUMOylation dynamics during cell-cycle progression reveals FoxM1 as a key mitotic SUMO target protein. Mol Cell 53, 1053–1066.
Shamu CE, Murray AW (1992). Sister chromatid separation in frog egg extracts requires DNA topoisomerase II activity during anaphase. J Cell Biol 117, 921–934.
Shcherbakova DM, Baloban M, Emelyanov AV, Brenowitz M, Guo P, Verkhusha VV (2016). Bright monomeric near-infrared fluorescent proteins as tags and biosensors for multiscale imaging. Nat Commun 7, 12405.
Spence JM, Phua HH, Mills W, Carpenter AJ, Porter AC, Farr CJ (2007). Depletion of topoisomerase IIalpha leads to shortening of the metaphase interkinetochore distance and abnormal persistence of PICH-coated anaphase threads. J Cell Sci 120, 3952–3964.
Sridharan V, Azuma Y (2016). SUMO-interacting motifs (SIMs) in Polo-like kinase 1-interacting checkpoint helicase (PICH) ensure proper chromosome segregation during mitosis. Cell Cycle 15, 2135–2144.
Sridharan V, Park H, Ryu H, Azuma Y (2015). SUMOylation regulates polo-like kinase 1-interacting checkpoint helicase (PICH) during mitosis. J Biol Chem 290, 3269–3276.
Stephan AK, Kliszczak M, Morrison CG (2011). The Nse2/Mms21 SUMO ligase of the Smc5/6 complex in the maintenance of genome stability. FEBS Lett 585, 2907–2913.
Wagner K, Kunz K, Piller T, Tascher G, Hölper S, Stehmeier P, Keiten-Schmitz J, Schick M, Keller U, Müller S (2019). The SUMO isopeptidase SENP6 functions as a rheostat of chromatin residency in genome maintenance and chromosome dynamics. Cell Rep 29, 480–494.e5.
Wang LH, Mayer B, Stemmann O, Nigg EA (2010). Centromere DNA decatenation depends on cohesin removal and is required for mammalian cell division. J Cell Sci 123, 806–813.
Wang LH, Schwarzbraun T, Speicher MR, Nigg EA (2008). Persistence of DNA threads in human anaphase cells suggests late completion of sister chromatid decatenation. Chromosoma 117, 123–135.
Whitehouse I, Stockdale C, Flaus A, Szczelkun MD, Owen-Hughes T (2003). Evidence for DNA translocation by the ISWI chromatin-remodeling enzyme. Mol Cell Biol 23, 1935–1945.
Xu X, Yanagida M (2019). Suppressor screening reveals common kleisin-hinge interaction in condensin and cohesin, but different modes of regulation. Proc Natl Acad Sci USA 116, 10889–10898.
Yau KC, Arnaoutov A, Aksenova V, Kaufhold R, Chen S, Dasso M (2020). RanBP1 controls the Ran pathway in mammalian cells through regulation of mitotic RCC1 dynamics. Cell Cycle 19, 1899–1916.
Yoshida MM, Ting L, Gygi SP, Azuma Y (2016). SUMOylation of DNA topoisomerase IIalpha regulates histone H3 kinase Haspin and H3 phosphorylation in mitosis. J Cell Biol 213, 665–678.
Zhang XD, Goeres J, Zhang H, Yen TJ, Porter AC, Matunis MJ (2008). SUMO-2/3 modification and binding regulate the association of CENP-E with kinetochores and progression through mitosis. Mol Cell 29, 729–741.
Zhu F, Gamboa M, Farruggio AP, Hippenmeyer S, Tasic B, Schule B, Chen-Tsai Y, Calos MP (2014). DICE, an efficient system for iterative genomic editing in human pluripotent stem cells. Nucleic Acids Res 42, e34.